Klinik für Kinder-Onkologie, -Hämatologie und klinische Immunologie, Universitätsklinikum Düsseldorf der Heinrich-Heine-Universität Düsseldorf

Direktor: Prof. Dr. Arndt Borkhardt

Mutational analysis of high-risk pediatric tumors

Dissertation

zur Erlangung des Grades eines Doktors der Medizin der medizinischen Fakultät der Heinrich-Heine-Universität Düsseldorf

vorgelegt von

Celine Chiu

2022

Als Inauguraldissertation gedruckt mit Genehmigung der Medizinischen Fakultät der Heinrich-Heine-Universität Düsseldorf

gez.:
Dekan: Prof. Dr. med. Nikolaj Klöcker
Erstgutachter: Prof. Dr. med. Arndt Borkhardt
Zweitgutachterin: Prof. Dr. med. Dagmar Wieczorek

For my family and friends who supported me.

Parts of this work have been published:

Chiu, C., Loth, S., Kuhlen, M., Ginzel, S., Schaper, J., Rosenbaum, T., Pietsch, T., Borkhardt A., Hoell, J., 2019, *Mutated SON putatively causes a cancer syndrome comprising high-risk medulloblastoma combined with café-au-lait spots*, Familial Cancer 18:353-35 [1]

Zusammenfassung

Die akute lymphatische Leukämie ist eine der häufigsten Krebserkrankungen im Kindesalter mit einer prinzipiell sehr guten Prognose. Jedoch gibt es Patienten, die beispielsweise aufgrund von schlechtem Ansprechen auf die initiale Therapie oder aufgrund eines aggressiven Subtyps der Erkrankung einen progredienten, therapierefraktären Krankheitsverlauf erleiden. Zusätzlich kann es nach initialer Remission zu einem Rezidiv der Erkrankung kommen, sodass eine allogene Stammzelltransplantation (allo-SCT) indiziert sein kann. Wenn ein weiteres Rezidiv nach allogener Stammzelltransplantation auftritt, ist das Gesamtüberleben mit nur etwa 8% sehr unbefriedigend. Diese multi-rezidivierenden Leukämien sind sehr aggressiv und aufgrund von dann limitierten Therapieoptionen schwierig zu behandeln. Bisher gibt es in solchen Fällen noch kein etabliertes Therapieregime. Eine zweite allogene Stammzelltransplantation kann durchgeführt werden, jedoch sollte vorher zumindest eine morphologische, besser eine molekulare Remission erreicht werden.

Auch wenn diese multi-rezidivierenden Leukämien sehr selten sind, ist es von essentieller Bedeutung, ihre Biologie zu verstehen und ihre genetischen Veränderungen zeitnah nach Diagnosestellung zu identifizieren, um individuelle Therapieansätze zu ermöglichen.

Um sich dieser Fragestellung zu nähern, wurde eine Gesamtexomsequenzierung der leukämischen Blasten von drei Kindern mit Rezidiv nach zweimaliger allogener Stammzelltransplantation durchgeführt, um das Mutationsspektrum zu jedem Stadium der Erkrankung (initiale Diagnose, erstes Rezidiv, Rezidiv nach allogener Stammzelltransplantation, Rezidiv nach zweiter Stammzelltransplantation) zu charakterisieren und um genetische Veränderungen zu identifizieren, die potentiell therapierbare Angriffspunkte darstellen.

Es konnte gezeigt werden, dass ALL-Rezidive nach zweiter allogener Stammzelltransplantationen sehr individuell sind und ein großer Unterschied auf Mutationsebene zwischen den Patienten besteht. Viele Mutationen sind nur

individuell auf einen Patienten beschränkt oder exklusiv für jede Stufe der Erkrankung, was die Plastizität der genetischen Veränderungen während der Leukämie-Progression betont. Dies hebt die Notwendigkeit hervor, bei jedem Patienten immer das aktuellste Leukämierezidiv für eine entsprechend angepasste Therapie zu untersuchen.

Zusätzlich konnte festgestellt werden, dass sogar im zweiten Rezidiv nach Stammzelltransplantation genetische Veränderungen gefunden werden konnten, die potentiell therapierbar sind. Wir validierten diese Mutationen mittels Sanger-Sequenzierung. Wir klonierten diese mutierten Gene in den Expressionsvektor PMC3, um zukünftige funktionelle Assays in BA/F3-Zellen zu ermöglichen.

Der folgende Abschnitt wurde publiziert in Chiu et. al 2019 [1]

Wie bereits erwähnt, ist die akute lymphatische Leukämie die häufigste Krebserkrankung im Kindesalter. Das Medulloblastom wiederum ist der häufigste bösartige Hirntumor im Kindesalter. Diese hochmaligne Neubildung tritt meist vor dem 10. Lebensjahr und häufiger bei Jungen auf. Die ereignisfreie 5-Jahres-Überlebensrate beim Medulloblastom mit hohem Risiko ist mit 62% trotz einer multimodalen Therapie mit chirurgischer Resektion, Bestrahlung und Chemotherapie unbefriedigend. Wir berichten über den Fall eines Jungen, der von konsanguinen Eltern geboren wurde. Auffallend war, dass er mehrere Café-au-lait-Flecken hatte. Im Alter von 3 Jahren wurde bei ihm ein metastasiertes Medulloblastom diagnostiziert. Der Patient starb nur 11 Monate nach der Diagnose eines fulminanten Rezidivs, das sich als meningeale und spinale Ausbreitung darstellte. Eine Ganzexom-Sequenzierung der Keimbahn-DNA wurde eingesetzt, um die diesem mutmaßlichen Krebssyndrom mit der Kombination von Medulloblastom und Hautveränderungen zugrunde liegende Mutation zu erkennen. Nachdem wir alle homozygoten Gen-SNVs gescreent hatten, identifizierten wir eine Mutation des Gens *SON*, eines essentiellen Proteins in der Zellzyklusregulation und der Zellproliferation, als wahrscheinlichste genetische Ursache.

Abstract

Acute lymphoblastic leukemia (ALL) represents the most frequent childhood cancer with a usually very favorable prognosis. However, there are patients, who suffer from treatment refractory disease of an aggressive subtype. In addition, a relapse of the disease can occur, so that an allogenic stem cell transplantation (allo-SCT) is indicated. If another relapse occurs after first allo-SCT, the overall survival rate is very poor (around 8 %). These multi-relapsed leukemias are very aggressive and difficult to treat with fairly limited therapeutic options. There are currently no established therapies available in this scenario. A second allo-SCT can be performed but only after at least a morphologic, better a molecular remission has been achieved.

Even though these multi-relapsed leukemias are very rare, it is of crucial importance to understand their biology and to detect leukemic mutations fast to enable individualized therapeutic approaches.

To address this clinical need, whole exome sequencing (WES) of leukemic blasts of three children with relapses following second allo-SCTs was performed to characterize the mutational spectrum at each step of the disease (initial diagnosis, first relapse, relapse after first allo-SCT, and relapse after second allo-SCT) and to identify genetic alterations that represent potentially druggable targets. We can show that ALL relapses after two allo-SCTs are highly individual displaying a high diversity between patients. Many mutations are patient-individual and/or exclusive to each step of the disease, which underlines the plasticity of genetic lesions during leukemia progression. That emphasizes the need to always analyze the most current relapse sample in every patient to find an appropriate therapy.

Additionally, even in the final relapses, alterations were identified, that are potentially treatable and described as malignant. These mutations were validated by Sanger sequencing. We cloned these mutated genes into the expression vector PMC3 to enable future functional assays in BA/F3 cells.

The following paragraph was published in Chiu et al., 2019 [1]:

As mentioned earlier, ALL represents the most frequent childhood cancer. As far as solid tumors are concerned, medulloblastoma is the most frequent malignant brain tumor in childhood. This highly malignant neoplasm occurs usually before ten years of age and more frequently in boys. The 5-year event-free survival rate for high-risk medulloblastoma is low at 62% despite multimodal therapy including surgical resection, radiation therapy and chemotherapy. We report the case of a boy, who was born to consanguineous parents. Prominently, he had multiple café-au-lait spots. At the age of three years, he was diagnosed with a high-risk metastatic medulloblastoma. The patient died only eleven months after diagnosis of a fulminant relapse presenting as meningeal and spinal dissemination. Whole-exome sequencing of germline DNA was employed to detect the underlying mutation for this putative cancer syndrome presenting with the combination of medulloblastoma and skin alterations. After screening all possible homozygous SNVs, we identified a mutation in *SON*, an essential protein in cell cycle regulation and cell proliferation, as the most likely genetic cause.

Abbreviations

Abbreviation	Long Term
ALL	Acute lymphoblastic leukemia
Allo-SCT	Allogeneic stem cell transplantation
Bp	Base pair
BSA	Bovine serum albumine
CGC	Cancer gene census
DNA	Desoxyribonucleic acid
g	Gram
L	Liter
mg	Miligram
min	Minute
mL	Milliliter
NGS	Next generation sequencing
OG	Oncogenome
PCR	Polymerase chain reaction
RNA	Ribonucleic acid
Rpm	Rotations per minute
sec	Second
SNV	Single nucleotide variation
WES	Whole exome sequencing
WGA	Whole genome amplification

Table of content

List of tables

List of figures

1 Introduction

1.1 The importance of whole-exome sequencing for high-risk tumor diseases

Current multimodal therapies of malignant tumors in childhood achieve a 5-year overall survival rate of about 80% across all tumors [2]. However, pediatric tumors that do not respond well to standardized therapies due to their high-risk profile remain problematic. In this context, therapy failure occurs resulting in disease process or a relapse. It is important to understand the genetic cause of highly malignant tumors in order to develop therapeutic strategies based on this knowledge. This was recently highlighted by the pilot project INFORM (Individualized Therapy for Relapsed Malignancies in Childhood). By rapid sequencing of the patient's genome corresponding mutations could be discovered, which could directly provide new therapeutic approaches for many patients [3, 4].

Here, whole exome sequencing (WES) in three pediatric patients with acute lymphoblastic leukemia (ALL) and one patient with medulloblastoma combined with café-au-lait spots was performed to analyze their genetic profiles.

1.2 Hematopoietic system and development of acute lymphoblastic leukemia

Hematopoiesis is the mechanism by which our body produces blood cells. This takes place in bone marrow (adults) or in spleen and liver (unborn children and infants). Basically, the hematopoietic system is divided into the lymphatic and the myeloid lineage. Blood cells develop from stem cells passing through differentiation and proliferation. T- and B-lymphocytes develop from lymphatic stem cells, while granulocytes, monocytes, thrombocytes and erythrocytes develop from myeloid stem cells (**Fig. 1**) [5].

During the development from a stem cell to a mature blood cell, many differentiation steps and cell divisions are necessary. In this process, alterations

in the genome may occur. When a mutation in a tumor driving gene occurs, there is an increased possibility that a preleukemic subclone develops. ALL is based on clonal expansion of lymphatic stem cells from T- or B-cell lineages (**Fig. 1**) [6].

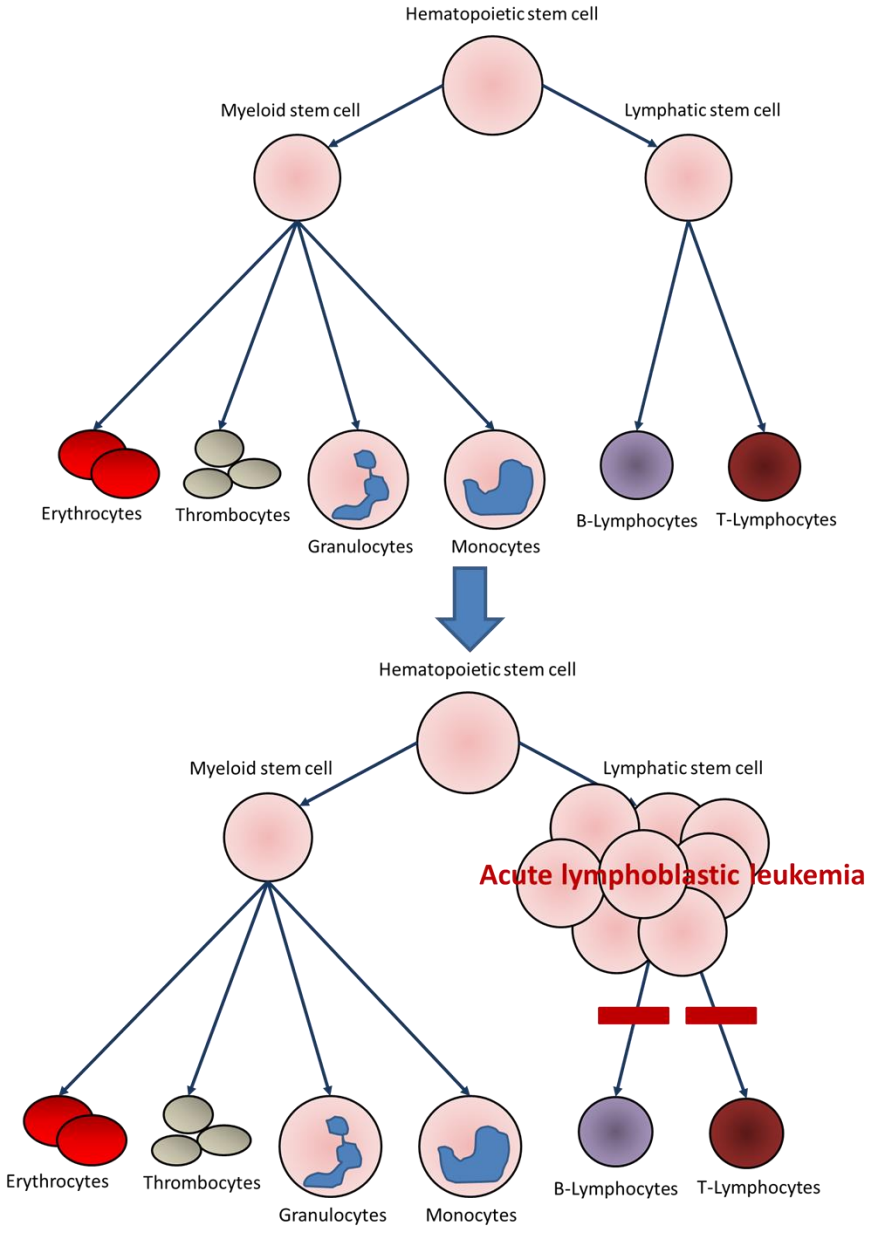

Fig. 1: Hematopoietic system and acute lymphoblastic leukemia. Schematic illustration of the hematopoietic system. Erythrocytes, thrombocytes, granulocytes and monocytes develop from myeloid stem cells, T- and B-Lymphocytes from lymphatic stem cells. When mutations occur in certain genes, lymphatic stem cells proliferate uncontrolled, which leads to acute lymphoblastic leukemia. Modified from Niemeyer et. al, 2017 [7].

1.3 Epidemiology and prognosis of pediatric acute lymphoblastic leukemia

Leukemia – a neoplastic disease of the hematopoietic system – represents with 30% the most frequent cancer in childhood, among which ALL is the most common subtype. Usually prognosis at the initial manifestation is good, as in 90% of the cases a long-term cure can be achieved [8]. However, there are patients, who relapse because of a poor response to initial therapy and/or an aggressive subtype, so that an allogeneic stem cell transplantation (allo-SCT) is indicated [9, 10]. After allo-SCT, if performed in complete remission, 70 to 75% of patients show a relapse-free survival [9, 10].

If another relapse occurs after first allo-SCT, the survival rate is poor. The EBMT (**E**uropean Society for **B**lood and **M**arrow **T**ransplantation) has reported an overall survival of 8% of ALL after allo-SCT relapse [11]. The main reason for this is that the leukemia then is likely a very aggressive one and is difficult to treat with standard therapies. There are no established therapies available in this clinical situation, which is in part due to cumulative toxicities of previous chemotherapies [12]. Therefore, an individualized therapeutic including immunotherapeutic approaches (if not previously already received by the patient) such as CD19/CD3-bispecific antibody blinatumomab [13], CAR-T-cells [14] or small molecule therapies are then called for. To offer those multi-relapsed patients an individualized treatment, we identified leukemia specific mutations by performing WES. Apart from identifying potentially therapeutically targetable lesions, we also improved understanding of the dynamic clonal evolution in leukemic blasts.

A second allo-SCT ideally after at least a morphologic remission has been achieved, is then usually performed [15]. Despite the fact that these cases are rare, it is of crucial importance to understand the biology behind these cases and to detect the leukemic mutations as fast as possible with WES, thereby ideally finding druggable targets to induce another remission [16].

1.4 Clonal evolution of leukemic blasts

The concept of clonal dynamics of the leukemic blasts describes the evolution of blast cells from one relapse to the next. Each time a leukemia develops, there are preceding mutations in the blast cells. That means that each step of a leukemia usually has its own mutational spectrum. Usually, there is one main clone, which is mainly driving the disease, and some sub-clones. But the main clone at the time of initial diagnosis does not have to be the main clone in the relapse. Another clone could have proliferated and be the reason for the relapse. The clone itself can change additionally by getting new mutations [17] (**Fig. 2**). Therefore, each step of the disease has to be treated as a new disease because the mutational spectrum might have significantly changed when compared to the last relapse. That means, that it is not sufficient to analyze the sample taken at initial diagnosis, but also all relapse samples, to find an adequate therapy.

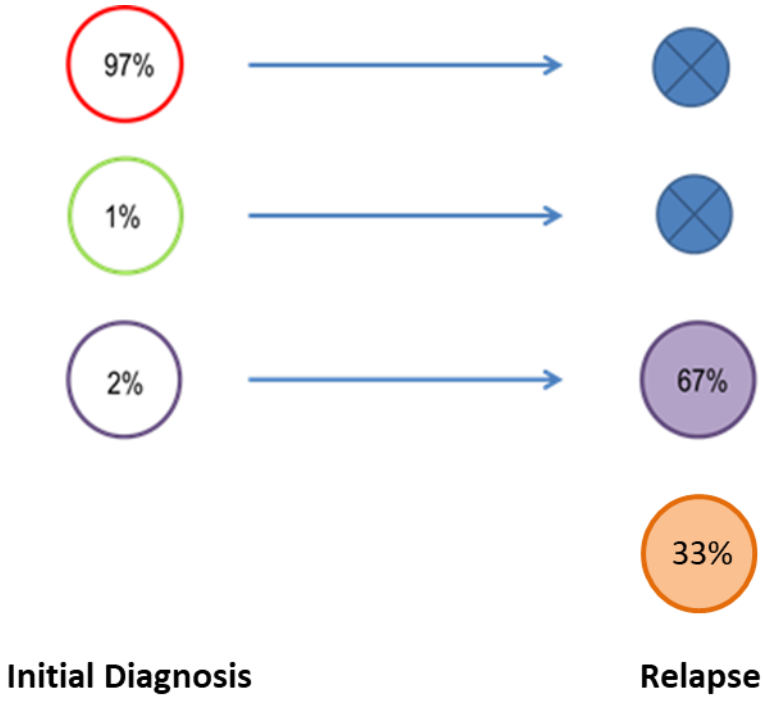

Fig. 2: Example of clonal evolution of leukemic blasts. Blast cells are shown as colored circles; percentage describes the percentage of blast clones during disease; blue painted circles show the clones that do not appear in relapse; violet painted circle shows the main clone during relapse changed by acquiring new mutations; orange painted circle shows a new clone during relapse. Modified from Greaves et al., 2012 [17].

1.5 Oncogenomes and driver mutations in cancer

We defined oncogenomes, which consist of single nucleotide variations (SNVs) with oncogenic effects. These SNVs are putatively involved in leukemogenesis. Genetic mutations of proto-oncogenes lead to development of oncogenes, so that gene regulation no longer functions properly and cells proliferate in an uncontrolled manner [18]. These mutations are also known as driver mutations. Mutations in driver genes affect a crucial switches in signal transduction pathways. The so-called oncogenome (OG) represents those genetic mutations that are specific for a tumor disease, in the here presented cases, leukemia-specific. Also, each step of the disease, whether initial or relapsed disease, has its own defining oncogenome. Usually tumor cells contain numerous somatic mutations, which often show no causal relationship to growth and proliferation of the tumor. These mutations are defined as passenger mutations and often occur because of repair errors during cell division. Unlike passenger mutations, the driver mutations show a direct causality to tumor development [19]. These driver mutations have to be identified to enable possible therapeutic options.

1.6 Calculation of oncogenomes and multi germline challenge

The oncogenomes, which describe the somatic alterations that are likely responsible for the leukemia and specific to each step of the leukemia, have to be calculated bioinformatically from the patients' samples. To only identify leukemia specific somatic variants, it is necessary to subtract germline variations from both the patient and the donor (if the patient has been transplanted already) (**Fig. 3**). Since our patients received two stem cell transplantations at the time of third relapse, we faced a challenge against multiple germlines. The two donor germline mutations and the patients' germline mutations have to be subtracted from the mutations found in the third relapse. Only then do we obtain a mutational spectrum that can only be related to leukemia, also called true somatic variants.

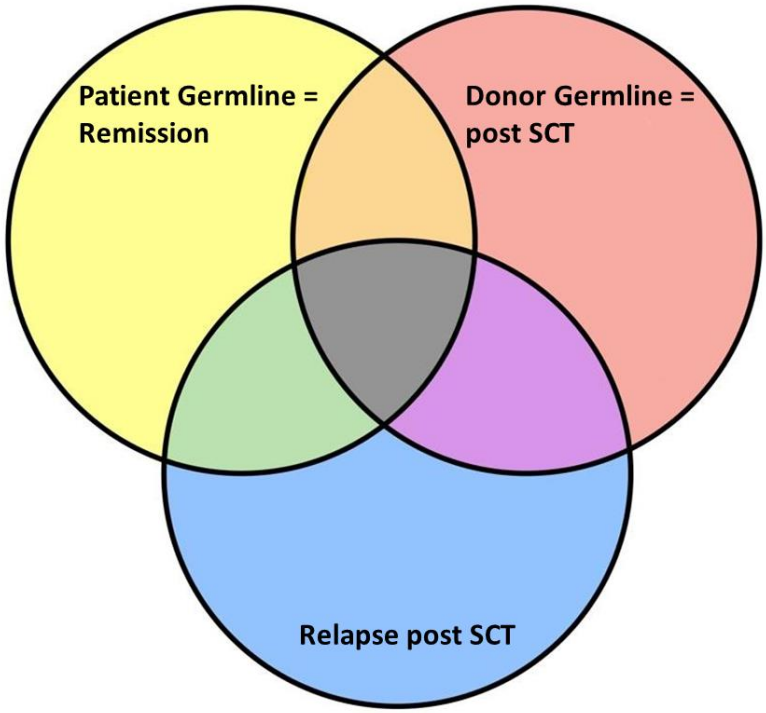

Fig. 3: Two germline challenge. The yellow circle represents the mutations of the patient germline. The red circle illustrates the mutations of the donor germline. The blue circle contains all mutations that are found in leukemia after SCT. However, only the area painted in blue is leukemia-specific, so that the overlapping mutational spectra must be subtracted.

1.7 Association between medulloblastoma in childhood and café-au-lait spots

The following paragraphs were published in Chiu et al., 2019 [1]

Medulloblastoma is the most frequent malignant brain tumor in childhood, representing around 20% of pediatric central nervous system tumor [20]. Usually, medulloblastoma occurs before 10 years of age and more frequently in boys [20-22]. The 5-year survival rate for high-risk medulloblastoma is low at about 50% despite multimodal therapy including surgical resection, radiation therapy and chemotherapy. Tumor dissemination at the time of diagnosis and relapse remain the main cause of therapeutic failure [23].

Whenever tumors are diagnosed at an uncommonly early age or are accompanied with additional features, an underlying genetic cancer susceptibility syndrome should be considered. Common cancer susceptibility syndromes include Li-Fraumeni syndrome (mutations in *TP53*), Costello syndrome (mutations in *HRAS* [24]), constitutional mismatch repair-deficiency (CMMR-D [25], and neurofibromatosis type 1 (mutations in *NF1* [26]). The latter typically presents with tumors of the nerval system, especially neurofibromas or low- and high-grade gliomas, and rarer malignant peripheral nerve sheath tumors (MPNST) and café-au-lait spots [27-29]. Other syndromes, in which brain tumors co-occur with skin alterations, include tuberous sclerosis [30, 31] and Sturge-Weber syndrome (all reviewed in [32]). However, cases of children with medulloblastoma are not usually combined with café-au-lait spots.

A rapid diagnosis of cancer syndromes is important for subsequent genetic counseling as well as potential treatment alterations. This might include not only adapting therapy regimens to reduce the administered doses of certain drugs but also limiting the exposure to radiation in case of an underlying increased radiosensitivity. Whole-exome sequencing (WES) has proven a useful tool in the detection of both inherited and acquired mutations [33].

The case of a three-year-old boy was investigated, who was diagnosed with a medulloblastoma and died of a fulminant relapse only eleven months after the initial tumor diagnosis. As he had consanguineous parents and skin features (**Fig. 4**) suspicious of an inherited syndrome, WES was employed to identify the underlying molecular defect.

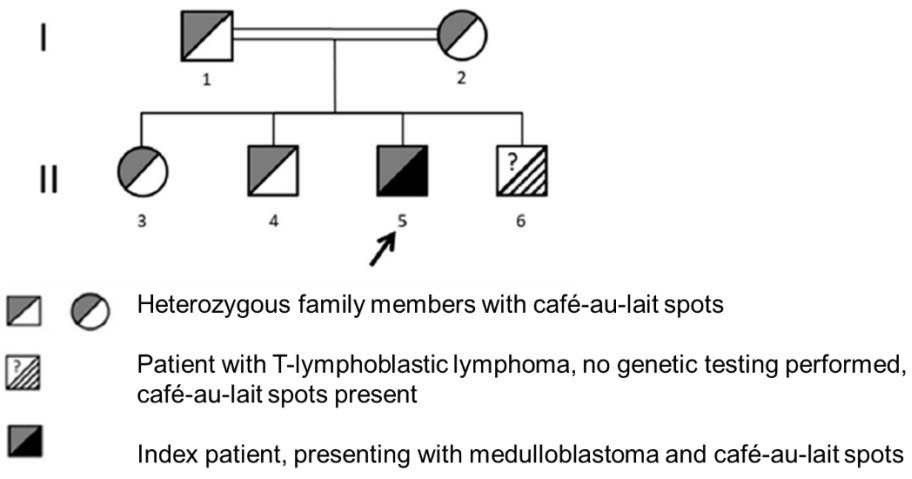

Fig. 4 Pedigree of the investigated family. Circles represent females and squares represent males. The black arrow indicates the index patient. Grey color marks a phenotype with café-au-lait spots and black color marks the occurrence of medulloblastoma. Reproduced from Chiu et al., 2019 [1].

1.8 Aim of the project

The aim of this project was to determine mutational spectra by performing WES of high risk pediatric tumor diseases such as ALL and medulloblastoma.

We wanted to characterize the plasticity of the mutational spectra from the initial leukemic diseases with a special focus on driver mutations and druggable targets. We also wanted to analyze, whether newly emerging mutations potentially increase the malignancy of the individual leukemias. Further we wanted to explore, how the relapse after second allo-SCT differs from the relapse after first allo-SCT. A thorough understanding of these fulminant leukemic relapses is paramount to provide those patients the best possible chances for targeted therapies.

Regarding the association between medulloblastoma and café-au-lait spots, we wanted to detect a genetic correlate, which could be responsible for this rare occurrence.

2 Materials and methods

2.1 Materials

2.1.1 Devices and consumables

All devices are listed in **Table 1**. Consumables, in particular disposable pipettes (2 ml, 5 ml, 10 ml and 25 ml) and filter systems (0.22 µm: 150 ml, 250 mL, 500ml were purchased from Corning (New York, USA), small reaction tubes (0.2 ml, 0.5 ml, 1.5 ml and 2,0 ml) from Eppendorf (Hamburg, Germany) and various sizes of pipette tips (10 µl, 20 µl, 100 µl, 200 µl and 1000 µl) were purchased from Starlab (Hamburg, Germany). Various sizes of scalpels (No. 10, 11 and 15) were purchased from Feather (Osaka, Japan).

Device	Company
Microscope (Axio Observer)	Carl Zeiss Microscopy, Jena, Germany
Allegra X-12 R Centrifuge	Beckman Coulter, Brea, USA
Centrifuge 5417 R	Eppendorf, Hamburg, Germany
Centrifuge 5403	Eppendorf, Hamburg, Germany
Multifuge Heraeus 3S R+	Thermo Scientific, Rockford, IL, USA
Centrifuge	NeoLab, Heidelberg, Germany
Nano Drop ND-1000 Spectrophotometer	Peqlab, Erlangen, Germany
Thermocycler GeneAmp PCR System 9700	Applied Biosystems, Thermo Scientific, Rockford, IL, USA
Thermocycler T Gradient	Analytik Jena, Jena, Germany
Biophotometer	Eppendorf, Hamburg, Germany
Biometra Low Voltage Power Supplies	Analytik Jena, Jena, Germany
Imager	Intas, Göttingen, Germany
UV Transluminator 2035	Herolab, Wiesloch, Germany
Shaking Incubator Certomat BS-T	Sartorius B. Braun, Wolf Laboratories, Pocklington, York, UK
Bacteria Incubator Heraeus	Thermo Scientific, Rockford, IL, USA
Vortex mixer VF2	IKA Labortechnik, Staufen, Germany

Milli-Q® Integral System	Millipore, Darmstadt, Germany
Ice System	Scotsman, Milan, Italy
Scale	Kern, Balingen-Frommern, Germany
Rolling Shaker SRT6	Stuart equipments, Staffordshire, UK
Certomat® BS-T Incubation shaker	Sartorius AG, Göttingen, Germany
Thermal Shaker	Eppendorf, Hamburg, Germany

Table 1: Devices. Used devices and corresponding companies are listed in the table.

2.1.2 Oligonucleotides

All oligonucleotides are listed in **Table 2 – 6**. Primers were designed with Primer 3 (v. 0.4.0) and ordered from MWG Biotech (Ebersberg, Germany).

Primer	Oligonucleotid sequence
NRAS-Fwd	5'-GGACAGGTTTTAGAAACT-3'
NRAS-Rev	5'-GCCCAAGGACTGTTGAAAAA-3'
DOT1L-Fwd	5'-TGAAGCCAAGAGGAGGATTG-3'
DOT1L-Rev	5'-CTCCCGGGTTCACATCATT-3'
DOT1L-nested-Fwd	5'-AACTCGCTTCCTGCCTCTC-3'
DOT1L-nested-Rev	5'-CCTGCCTCCACCTGTTTTT-3'
CREBBP-Fwd	5'-CTCCAACTGTGCTGCTCTCA-3'
CREBBP-Rev	5'-GGAGAAGTGTTGCAGGGCTA-3'
NRG2-Fwd	5'-CATTCCCATGAGGAACCATC -3'
NRG2-Rev	5'-GGAGAAAAGGGATGGAAAGG-3'
MET-Fwd	5'-TAGAAGAGCCCAGCCAGTGT-3'
MET-Rev	5'-TCAGGCTGGCTCCTATTTGT-3'
VHL-Fwd	5'-GCGGAGAACTGGGACGAG-3'
VHL-Rev	5'-GAATGCTCTGACGCTTACGA-3'
KRAS-Fwd	5'-CCCTGACATACTCCCAAGGA-3'
KRAS-Rev	5'-CTTAAGCGTCGATGGAGGAG-3'
MLL2-Fwd	5'-GAGAGTCGGTCATCGCTAGG-3'
MLL2-Rev	5'-CACCTCTCCTGTCGAAAAGC-3'
MITF-Fwd	5'-TCCTGTCACCTCTTGATTTTCA-3'
MITF-Rev	5'-GGAACATTGACTCCCACCAT-3'

Table 2: Primers for Sanger sequencing validation. Listed primers were used to validate WES data with Sanger sequencing.

Primer	Oligonucleotid sequence
NRAS_klon_fwd	5'-ACGCACGCGT GCCACCATGACTGAGTACAAACTG-3'
NRAS_klon_Rev	5'-ACGCGTCGAC CATCACCACACATGGCAA-3'
KRAS_klon_fwd	5'-ACGCACGCGTGCCACCATGACTGAA TATAAACTTGTGGTAG-3'
KRAS_klon_Rev	5'-ACGCGTCGAC CATTATAATGCATTTTTTAATTTTC-3'
MET_klon_fwd	5'-ACGCAAGCTTGCCACC ATGAAGGCCCCCGCTGTG -3'
MET_klon_rev	5'-ACGCACGCGT TGATGTCTCCCAGAAGGA -3'

Table 3: Primers to amplify genes of interest from cDNA. Blue colored sequence indicates the adhesion-sequence for restriction enzymes; Violet colored sequence indicates the Kozak-sequence; green colored sequence indicates the palindromic cutting sequence; yellow colored sequence indicates start and end of the gene.

Primer	Oligonucleotid sequence
NRAS_muta_fwd	5'-GTTGGAGCAGcTGGTGTTGGG-3'
NRAS_muta_Rev	5'-CACCACCAGTTTGTACTC-3'
MET_muta_fwd	5'-TACTTCTTGAtGGTCCAAAGG-3'
MET_muta_Rev	5'-AATAAAATTGTTGCTTTCAAAG-3'
KRAS_muta_fwd	5'-AGTTGGAGCTaGTGGCGTAGG-3'
KRAS_muta_rev	5'-ACCACAAGTTTATATTCAGTCATG-3'
MET_actmut_fwd	5'-GTGAAGTGGAcGGCTTTGGAAAG-3'
MET_actmut_rev	5'-TGGCAGCTTTGCACCTGT-3'
MET_actmut_b3_fwd	5'-GTAAGCCCAAtTACAGAAATGG-3'
MET_actmut_b3_rev	5'-ACTTCGGGCACTTACAAG-3'
NRAS_actmut_fwd	5'-GTTGGAGCAGaTGGTGTTGGG-3'
NRAS_actmut_rev	5'-CACCACCAGTTTGTACTCAG-3'
KRAS_actmut_fwd	5'-GTTGGAGCTGtTGGCGTAGGC-3'

KRAS_actmut_rev	5'-TACCACAAGTTTATATTCAGTCATGG-3'

Table 4: Primers for mutagenesis. Lower case letter indicates the changed nucleotide.

Primer	Oligonucleotid sequence
Pmc_fwd	5'-CTCCATAGAAGACACCGGGAC-3'
Pmc_rev	5'-TGGGTACAACCCCAGAGC-3'
NRAS_Seq1	5'- AACCTCTACAGGGAGCAGAT-3'
KRAS_Seq1	5'-CACCATTATAGAGAACAAAT-3'
MET_Seq1	5'-ACATGGCTCTAGTTGTCGAC-3'
MET_Seq2	5'-TACATTGATGTTTTACCTGA-3'
MET_Seq3	5'GCCAGATTCTGCCGAACCAA-3'
MET_Seq4	5'-TTTCTCGATCAGGACCATCA-3'
MET_Seq5	5'-TGTGGCTGGGACTTTGGATT-3'
MET_Seq6	5'-AAGTGTGTCAAACAGTATTC-3'
MET_Seq7	5'-TCTGTTGTACCACTCCTTCC-3'
MET_Seq8	5'-TCTTCAACCGTCCTTGGAAA-3'
MET_Seq9	5'-CCCCATCCTAACTAGTGGGG-3'
MET_Seq10	5'-GTGAAGGGTCTCCGCTGGTG-3'
MET_Seq11	5'-GTGTGGTCCTTTGGCGTGCT-3'
MET_Seq12	5'-ACCAGCCTCCTTCTGGGAGA-3'

Table 5: Primers to sequence the cloned vector. Listed primers were used to perform Sanger Sequencing with the cloned vector.

Primer	Oligonucleotid sequence
SON_SNV_fwd	5'-TACCAGAGCCACCTGTGATG-3'
SON_SNV_rev	5'-ATCGTTGACAGCTCCGATGT-3'

Table 6: Primers for SNV Sanger sequencing of SON. The oligonucleotides were used for PCR-amplification and Sanger sequencing of the SNV in exon 3 of SON. Information of this table was published in Chiu et al [1].

2.1.3 Restriction enzymes

All used fast-digesting restriction enzymes are listed in **Table 7** and were ordered from Thermo Scientific (Rockford, IL, USA).

Cloned Genes	Restriction Enzymes	Palindromic sequence
NRAS	Mlu I	5'-A^CGCGT-3'
	Sal I	5'-G^TCGAC-3'
KRAS	Mlu I	5'-A^CGCGT-3'
	Sal I	5'-G^TCGAC-3'
MET	Mlu I	5'-A^CGCGT-3'
	Hind III	5'-A^AGCTT-3'

Table 7: Restriction enzymes. Listed restriction enzymes were used to cut cloning vectors.

2.1.4 Kits

All used kits are listed in **Table 8**.

Kits	Company
REPLI-g® UltraFast Mini Kit	Qiagen, Hilden, Germany
Phusion High-Fidelity DNA Polymerase	Thermo scientific, Rockford, IL, USA
Superscript® II Reverse Transcriptase	Invitrogen, Thermo Scientific, Rockford, IL, USA
miRNeasy® Mini Kit	Qiagen, Hilden, Germany
QIAshredder™	Qiagen, Hilden, Germany
AllPrep® DNA/RNA/miRNA Universal Kit	Qiagen, Hilden, Germany
QIAquick® Gel Extraction Kit	Qiagen, Hilden, Germany
Monarch® Plasmid Miniprep Kit	New England Biolabs, Ipswich, USA
Tag PCR Core Kit	Qiagen, Hilden, Germany
NucleoBond® Xtra Maxi EF	Machery-Nagel, Düren, Germany
Q5® Site-Directed Mutagenesis Kit	New Enland Biolabs, Ipswich, USA

Table 8: Kits.

2.1.5 Buffer and gel

Buffer and gel are listed in **Table 9**.

Buffer/Solution	Composition/ Company
50x TAE buffer	Bio Rad, Hercules, California, USA
Agarose Gel	• 1% Agarose • 100 ml TAE buffer

Table 9: Buffer and gel.

2.1.6 Chemicals

All chemicals are listed in **Table 10**.

Cheicals	Company
6X DNA loading dye	Thermo Scientific, Rockford, IL, USA
Agarose	Biozym, Hessisch Oldendorf, Germany
Ampicillin	Thermo Scientific Rockford, IL, USA
Ethidiumbromid	SIGMA-ALDRICH, St. Louis, USA
GeneRuler 1kb ladder	Thermo Scientific, Rockford, IL, USA
Gel Pilot 100bp ladder	Qiagen, Hilden, Germany
Isopropanol	VWR, Radnor, USA
LB-Medium (Lennox)	Carl Roth, Karlsruhe, Germany
LB-Agar (Lennox)	Carl Roth, Karlsruhe, Germany
Nuclease-free water	Thermo Scientific, Rockford, IL, USA

Table 10: Chemicals

2.2 Methods

2.2.1 Sample acquisition of medulloblastoma patient

The following paragraph was published in Chiu et al., 2019 [1]

Genomic DNA was isolated from peripheral blood obtained from the index case, the siblings as well as the parents. The AllPrep DNa/RNA Mini Kit (Qiagen, Hilden, Germany) was used to purify DNA according to manufacturer's instructions. The study was approved by the local ethics committee (study number 4489) and written informed consent was given by parents.

2.2.2 Exome library preparation, next generation sequencing and bioinformatic samples processing

Nucleid acids were extracted using AllPrep DNA/RNA Mini Kit (Qiagen, Hilden, Germany). Exome library preparation was performed as detailed in Hoell et al., 2014 [34]. Briefly, a modified Agilent SureSelectXT Human All Exon V4 + UTR kit was employed and 2 x 100 bp sequencing with a 6 bp index read was performed using the TruSeq™ SBS Kit v5+UTR on the HiSeq™ 2500 (Illumina, San Diego, California, USA). Exome library sequencing, next generation sequencing and bioinformatic sample processing had already been performed prior to the start of the below-mentioned experiments, which form part of the thesis.

2.2.3 Bioinformatic analysis

2.2.3.1 DNA data processing

Bioinformatic analysis was performed as described in Hoell et al, 2019 [35]. BcltoFastq1.8.2 (Illumina) was used to create the Fastq files. To adapt sequence data to the human reference genome (GRCh37), BWA version 0.6.1-r104 [36] with standard parameters was chosen. Samtools [37] was used to perform the conversion steps. Next, duplicate reads were removed [38, 39]. GATK [40] enable local realignment around indels, SNV-calling, annotation and recalibration. HapMap, OmniArray and dbSNP135 datasets that were allocated by the Broad Institute [41] were used for recalibration. Variant Effect Predictor [42] annotated the resulting variant calls using the Ensembl database (v70), which were then imported into an in-house MySQL database. This facilitated automatic and manual annotation, reconciliation and data analysis based on complex database queries. Loss of function prediction scores for PolyPhen2 [43] and SIFT [44] were obtained from the same Ensemble release. For the medulloblastoma patient, sequence variants within protein coding genes that are observed with less than 1% frequency in the 1000 genomes and ExAC project were considered for further analysis. Bioinformatic analysis was performed by Dr. Sebastian Ginzel (Department of Pediatric Oncology, Hematology and Clinical Immunology, University Children's Hospital Düsseldorf; Department of Computer Science, Bonn-Rhein-Sieg University of Applied Science, Sankt-Augustin).

2.2.3.2 Computation of oncogenomes

Oncogenomes were computed from the variant calls using MuTect [45] and VarScan2 [46]. SNVs were kept for further analysis only if they met the following criteria: covered at least 10x in all samples of a patient set; had a general minor allele frequency (GMAF) of less than 1%; and were mapped to canonical transcripts. The datasets were compiled and analyzed using R. Genes associated with DNA Polymerase function and Fanconi anemia were extracted from the gene families 'Fanconi anemia complementation groups (FANC)' and 'DNA polymerases (POL)' from HGNC database [47].

2.2.4 Whole genome amplification

Patients' samples were amplified by whole genome amplification with REPLI-g® UltraFast Mini Kit (Qiagen), which was performed according to manufacturer's specifications.

2.2.5 Gel electrophoresis

For electrochemical separation of DNA fragments, agarose gel electrophoresis was performed with 1% agarose gel (Biozym). To visualize the DNA, ethidium bromide (Sigma Aldrich) 1:10000 was added to the gel (5 µL of 10mg/ml ethidium bromide was added to 50 mL agarose solution). To estimate the size of the DNA fragments Gene Ruler 100 bp- or 1 kbp-DNA-Marker (Invitrogen) was used. To stain the sample, 6x loading dye (Thermo Scientific) was used. Electrophoresis was performed at 100 V in 1x TAE buffer (Bio Rad). UV light was applied for the detection of DNA.

2.2.6 Gel extraction

The DNA bands were excised using a clean scalpel and the DNA in agarose was placed into a sterile 1.5 mL Eppendorf tube. For purification of DNA, QIAquick Gel Extraction Kit (Qiagen) was used and the DNA was extracted according to manufacturer's instructions. DNA was eluted from column in 50 µL EB buffer and stored at -20°C.

2.2.7 Polymerase chain reaction (PCR)

To amplify a target fragment of DNA, PCR was performed using Phusion Polymerase (Thermo Fisher Scientific). Reaction setup (50 µL) contained the following components:

gDNA or cDNA	50-250 ng
5x Phusion HF buffer/GC buffer	10 µL
10 mM dNTPs	1 µL
Primer 1 (10 pmol/µL)	2.5 µL
Primer 2 (10 pmol/µL)	2.5 µL
Phusion Polymerase (Thermo Scientific)	0.5 µL
Nuclease Free Water	to 50 µL

Reaction setup (20 µL) for optimization reactions of amplification with Phusion Polymerase (Thermo Scientific) contained the following components:

cDNA (DHL4 or HEK)	25-125 ng
10x Phusion HF buffer/ GC buffer	4 µL
10 mM dNTPs	0.4 µL
Primer 1 (10 pmol/µL)	1 µL
Primer 2 (10 pmol/µL)	1 µL
Phusion Polymerase	0.2 µL
(if necessary) $MgCl_2$	0.08 µL
Nuclease Free Water	to 20 µL

The amplification was performed using the following PCR program:

1) 98° C, 30 sec
2) 98° C, 10 sec
3) 55 bis 65° C, 30 sec
4) 72° C, 30 sec/kb (when using gDNA)
5) 29 repeats of steps 2 to 4
6) 72° C, 7 min
7) 4°

Reaction setup (25 µL) for amplification using Taq polymerase (Qiagen) contained the following components:

gDNA	20 ng
10x Taq buffer	2.5 µL
10 mM dNTPs	0.5 µL
Primer 1 (10 pmol/µL)	0.5 µL
Primer 2 (10 pmol/µL)	0.5 µL
Taq-Polymerase (Qiagen)	0.1 µL
Nuclease Free Water	to 25 µL

The amplification was performed using the following PCR program:

1) 94° C, 2 min
2) 94° C, 30 sec
3) 65° C – 1° C, 30 sec
4) 72° C, 30 sec
5) 10 repeats of steps 2 to 4
6) 94° C, 30 sec
7) 55° C, 30 sec
8) 72° C, 30 sec
9) 24 repeats of steps 6 to 8
10) 4° C

2.2.8 Determination of concentration and purity of DNA and RNA

To determine the concentration and purity of DNA and RNA NanoDrop® ND-1000 Spectrophometer (Thermo Scientific) was used. For each measurement, 1 µL of RNA or DNA sample was applied. The RNA and DNA concentration was determined by absorption measurement at 260 nm wavelength. Additionally, the NanoDrop® Spectrophotometer offers the possibility of a graphical representation of the absorption spectrum within the wavelengths from 220 nm to 350 nm. In this wavelength range, substances affecting the absorption measurement such as solvents and protein contaminants of the isolated RNA or

DNA can be detected. The absorbance quotient A260/280 of pure RNA or DNA should be in the range of 1.9 to 2.1.

2.2.9 Sanger sequencing

Selected SNVs from exome sequencing were validated by Sanger sequencing. Sequencing was performed by Genomics & Transcriptomic Labor (GTL) of BMFZ (Düsseldorf, Germany).

2.2.10 RNA preparation

To purify RNA, Allprep DNA/RNA/miRNA Universal Kit (Qiagen) was used and RNA was extracted according to manufacturer's instructions. RNA was eluted in 30 µL RNAse free water and stored at -80°C.

2.2.11 cDNA synthesis

First-strand cDNA was synthesized from total RNA and fractioned RNAs using Superscript II (Invitrogen). Reaction setup contained the following components:

50 µM Oligo(dT)$_{20}$ Primer (Invitrogen)	1 µL
10 mM dNTPs	1 µL
RNA	1.5 µg
Nuclease Free Water	to 13 µL

The reaction setup was incubated for 5 min at 60°C. Afterwards the mixture was placed on ice for 1 min and the following components were added:

5x First-Strand Buffer	4 µL
0.1 M DTT	1 µL
RNAse Out (40 units/µL)	1 µL

Finally, the mixture was incubated 60 min at 50°C and 15 min at 70°C.

2.2.12 Enzyme restriction digestion

Purified cDNA and plasmids were cut by fast digestion restriction enzyme (New England Biolabs) before gel electrophoresis. The reaction setup (20 µL) contained the following components:

DNA	0.2 µg – 1 µg
10x Fast Digest Green buffer	2 µL
Restriction enzyme 1	1 µL
Restriction enzyme 2	1 µL
Nuclease Free Water	to 20 µL

The mixture was incubated for 5 min at 37°C.

2.2.13 Mutagenesis

Mutagenesis was performed using Q5® Site-Directed Mutagenesis Kit (New England Biolabs).

The reaction mixture consisted of:

Q5 Hot Start High-Fidelity 2x Master Mix	12.5 µL
Primer 1 (10 pmol/µL)	1.25 µL
Primer 2 (10 pmol/µL)	1.25 µL
DNA	1-25 ng
Nuclease Free Water	to 25 µL

Amplification was performed using the following PCR program:

1) 98° C, 30 sec
2) 98° C, 10 sec
3) 56-64° C, 30 sec/kb
4) 24 repetitions of steps 2 to 4
5) 72° C, 2 min
6) 4° C

To ligate the product the following reaction setup was used:

PCR-Product	1 µL
KLD Reaction Buffer	5 µL
KLD Enzyme (10x)	1 µL
Nuclease Free Water	to 10 µL

The mixture was incubated for 5 min at room temperature. Five µL were used for transformation into Escherichia coli (E. coli).

2.2.14 Production of chemically competent cells

To produce chemically competent cells, 100 mL of LB medium were inoculated with 1.5 mL of a fresh overnight culture of E. coli (Invitrogen). This cell suspension was incubated at 37°C and 250 rpm. At an absorption value between 0.4 and 0.5 (λ=600), the suspension was incubated on ice for 10 min. The medium was centrifuged at 5000 g for 10 min. Afterwards the cell pellet was resuspended in 40 mL TFB1 buffer. After 10 min incubation on ice, the buffer was spun down at 500 g for 10 min. The cell pellet was resuspended in 4 mL TFB2 buffer. One hundred µL aliquots were shock frozen in liquid nitrogen and then stored at -80°C. To evaluate the competency, a transformation with 1 pg/10 pg pUC19 was performed and the colony-forming units/µg used plasmid were determined.

2.2.15 Retransformation

For *in vivo* amplification of plasmids, competent E. coli (Invitrogen) were thawed on ice for about 20 min. One ng of plasmid solution was added to the cell suspension, which was incubated on ice for 30 min. Afterwards the mixture was incubated 30 sec at 42 °C and placed on ice. Then, 250 µL prewarmed LB medium was added and incubated for 1 h at 300 rpm at 37°C. The whole cell suspension was plated on ampicillin-containing plates with amounts of 20 µL to 200 µL and incubated overnight at 37°C. Colonies could be picked and further cultivated in LB medium.

2.2.16 Cloning

Bacteria

To amplify plasmids competent E. coli (Invitrogen) were used.

Culture conditions

Bacteria were cultivated at 37°C.

Culture medium for bacteria

To cultivate bacteria, LB agar plates (Lennox) and LB medium (Lennox) were used. To select transformed bacteria, Ampicillin (100 µg/mL) was added to the agar plates.

2.2.17 Plasmid preparation

For extracting plasmids from bacteria, the Monarch Plasmid Miniprep Kit (New England Biolabs) and the NucleoBond Xtra EF plasmid purification Kit (Machery Nail) were used according to the manufacturer's instructions.

3 Results

3.1 Cohort of three patients relapsing with ALL following two stem cell transplantations

All three patients 202, 705, 337 (1 female, 2 males) (Table 11) were enrolled in multicenter pediatric ALL trials. All cases were either treated according to NHL-BFM 90 or COALL protocols at initial diagnosis, followed by ALL-REZ BFM and ALL-SCT BFM 2003 protocols (except for patient 337 who was enrolled in the TCRalpha/beta-Haplo2010 trial) for stem cell transplantation. For first SCT, two patients received a matched-unrelated donor transplant and one patient was transplanted with bone marrow from his HLA-haploidentical mother. Following post SCT relapse, haploidentical SCT was performed in two of the three patients after morphological remission, in patient 337 allogeneic unrelated SCT was performed (as he had been receiving a haploidentical transplant after first relapse). Mean age at first diagnosis was 3.0 years (range 0.6-5.7 years), mean time from first diagnosis to first relapse (relapse before allo-SCT) was 3.8 years (range 1.8-6.7 years), mean time from initial diagnosis to relapse post first allo-SCT was 8.9 years (range 3.1-4-7 years) and mean time from first diagnosis to relapse after second allo-SCT was 10,4 years (range 4.3-21.2 years). Time from both SCT to corresponding post-allo-SCT relapses was short. Mean time from first SCT to relapse was 1.2 years (range 0.7.-1.9 years) and from second SCT to relapse was 0,6 years (range 0.3-1.0 years).

Due to the lack of standardized protocols, treatment following post-allo-SCT relapses varied considerably. At the time of this thesis, none of the three patients is alive, showing the poor prognosis of children suffering post-allo-SCT relapses. Please refer to **Table 11 and 12** for further details.

Patient ID	705	202	337
Sex	m	f	m
Age at first disease (yr)	0.6	5.7	2.8
Immunophenotype	prä-prä-B-ALL/Pro-B-ALL	cALL	cALL
CNS status	CNS negative	CNS negative	CNS negative
Age at relapse (yr)	7.3	7.5	5.9
Time to relapse (yr)	6.7	1.8	3.1
Age at SCT (yr)	17.8	8.1	6.3
MRD before SCT	BM neg. (morph.)	<1x10^-3-1x10^-4	<1x10^-4
Time to relapse after SCT (yr)	1.9	0.7	1.2
Age at 2nd SCT (yr)	19.8	9.4	7.9
MRD before 2nd SCT	BM neg. (morph.)	n/a	BM neg. (morph.)
Age at relapse after 2nd SCT (yr)	20.8	9.7	8.3
Time to relapse after 2nd SCT (yr)	1.0	0.3	0.4
Survival status	dead	dead	dead

Table 11: Patient details. M indicates male; f, female; neg., negative; BM, bone marrow; morph., morphologic; Morphological remission means < 5 % blasts in the BM and no extramedullary involvement; CNS, central nervous system; CNS status means detection of malignant cells in the cerebrospinal fluid; n/a, not available; SCT, stem cell transplantation; MRD, minimal residual disease; yr, year/years.

3.1.1 Clinical characteristics of the three patients

Patient ID	705	202	337
Sex	m	f	m
Age at first diagnosis of disease (in years)	0,6	5,7	2,8
Immunophenotype at first disease	pre-pre-B-ALL/pro-B-ALL	common ALL	common ALL
Cytogenetics (translocations, deletions etc.) at first disease	no metaphases found (Giessen)	BCR-ABL / TEL-AML1 / MLL-rearrang. / TCF3-PBX1 neg.	BCR-ABL / TEL-AML / MLL rearrang. / IgH rearrang. neg.
Chromosomal abnormalities (hypo-/hyperdiplod etc.) at first disease	no metaphases found (Giessen)	not evaluable	52,XY+X+6+14+17+21+21[12]/46,XY[6]
CNS disease / status at first disease	CNS negative	CNS negative	CNS negative
treatment protocol at first disease	NHL-BFM 90	CoALL	CoALL
risk category at first disease	n/a	LR intensified	HR
Age at relapse (in years)	7,3	7,5	5,9
Type of relapse (BM, CNS, other extramedullary)	BM	BM	BM
Treatment protocol at relapse	ALL-Rez-BFM	ALL-REZ BFM 2002	ALL-REZ BFM 2002
Immunophenotype at relapse	Pro-B-ALL with bilinear population	common ALL	common ALL
Cytogenetics (translocations, deletions etc.) at relapse	BCR-ABL, TEL-AML1 und MLL-rearrangements negativ	negative	no translocations
Chromosomal abnormalities (hypo-/hyperdiplod etc.) at relapse	47-49 XY	n/a	52,XY+X,t(2,10)(p12;q25)+6,i(7)(q10), +14+17+21+21[7/14]
CNS disease / status at relapse	CNS negative	CNS negative	CNS negative
Risk category at relapse	S2	S3	S3
Age at SCT (in years)	17,8	8,1	6,3
Study for transplant	ALL-SCT	ALL-SCT	TCRalpha/beta-Haplo2010
MRD before SCT/ Disease status at transplant	BM neg. (morph.)	$<1x10^{-3}$-$1x10^{-4}$	$<1x10^{-4}$
Type of SCT performed (MD, MSD, haploidentical)	unrelated, PBSC	MD	haploidentical (mother)
Type of conditioning regimen	TBI, Etoposide, ATG	Etoposide, ATG, TBI	Fludarabine/Thioguanine/Melphalan/ATG

Transplant center	Düsseldorf	Düsseldorf	Düsseldorf
HLA match	10/10	10/10	haploidentical (mother)
Sex of donor	f	m	f
Time to relapse (in years) after SCT	1,9	0,7	1,2
Type of relapse (BM, CNS, other) after SCT	BM, extramed. (kidney)	BM	BM
Immunophenotype at relapse after SCT	prä/pro-B-ALL	common ALL	common ALL
Cytogenetics (translocations, deletions etc.) at relapse after SCT	n/a	n/a	no translocations
Chromosomal abnormalities (hypo-/hyperdiplod etc.) at relapse after SCT	n/a	n/a	52,XY+X,t(2,10)(p12;q25)+6,i(7)(q10), +14+17+21+21[2/20]
CNS disease / status at relapse after SCT	CNS negative	n/a	CNS negative
Treatment at relapse after SCT	Fludarabine, Cyclophosphamide, Asparaginase, Mab-Campath+intrathecal therapy	Mab-Campath, PEG-Asparaginase, Fludarabine, Cyclophosphamide, Blinatumomab, Doxorubicin, Vincristine	Blinatumomab
Age at 2nd SCT (in years)	19,8	9,4	7,9
MRD before 2nd SCT	BM neg. (morph.)	n/a	BM neg. (morph.)
HLA match	haploidentical (father)	haploidentical (mother)	10/10
Sex of donor	m	f	m
Time to relapse (in years) after 2nd SCT	1,0	0,3	0,4
Treatment at relapse after 2nd SCT	ATG, Fludarabine, Thiotepa, Melphalan	n/a	Mercaptopurine, Methotrexat
Survival status	dead	dead	dead

Table 12: Clinical characteristics of the analyzed patients. M indicates male; f, female; neg., negative; BM, bone marrow; CNS, central nervous system; n/a, not available; SCT, stem cell transplantation; MD, matched donor; MSD, matched sibling donor; PBSC, peripheral blood stem cells; MRD, minimal residual disease; TBI, total body irradiation; ATG, Anti-Thymocyte Globulin. Modified from Hoell et al., 2019 [35].

3.1.2 Leukemia patient samples

All three patients were enrolled in multicenter pediatric ALL trials (ALL-REZ BFM 2002, CoALL, NHL-BFM 90) and the ALL-REZ BFM registry. The treatment

studies, the registry and the concomitant research were all approved by the respective institutional review boards and informed consent was obtained from all patients (and/or in case of children from their legal guardians). The ethic committee vote number is 3993.

Seven samples per patient were considered for this project. Those consisted of a sample at the time of initial diagnosis, the first remission after chemotherapy (representing the patient's germline), the first relapse after chemotherapy, the remission sample after first SCT (representing the first donor's germline) and the relapse after the first SCT, the remission sample after the second SCT (representing the second donor's germline) and the relapse after the second SCT (**Fig. 5**). However, only for one patient all seven samples were available (337). Two patients (202, 705) were missing the sample for initial diagnosis, so only six samples were available for them.

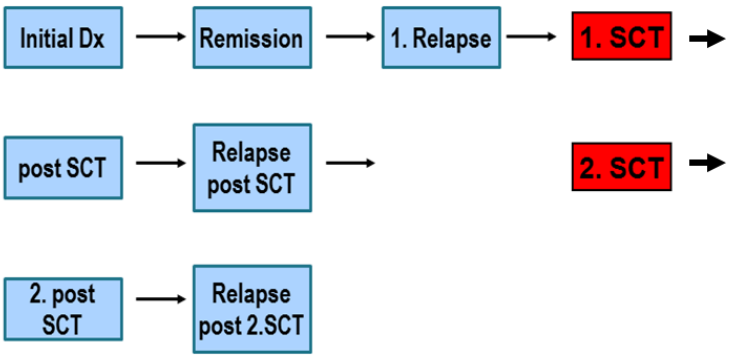

Fig. 5: Patient samples. Available patient samples (in blue) are shown in chronological order.

3.2 Calculation of oncogenomes

Since post-allo-SCT relapses usually occur in a situation of hematopoietic chimerism, two genetic germline backgrounds (donor and recipient) were subtracted bioinformatically to reveal mutations specific to the post-allo-SCT relapses (**Fig 6**).

In oncogenome 1, we show the somatic mutations that are responsible for the initial diagnosis of ALL. For this, mutations found at remission are subtracted from those found at initial diagnosis, so that leukemia-independent mutations are not

considered. Samples at the time of initial diagnosis were not available for two patients (202, 705), so no OG1 could be calculated for these two.

In oncogenome 2, we present the somatic mutations that occurred during the first relapse after chemotherapy, also by subtraction of the remission sample from the relapse sample.

In oncogenome 3 the donor germline and the patient germline must be subtracted from all variants found in the second relapse sample in order to identify only the leukemia specific mutations of the second relapse. Here, we have the challenge to consider two – the patients and the donor's – germlines.

Oncogenome 4 is calculated by subtracting variants of the two donor germlines and the patients' germline variants from the relapse after second SCT.

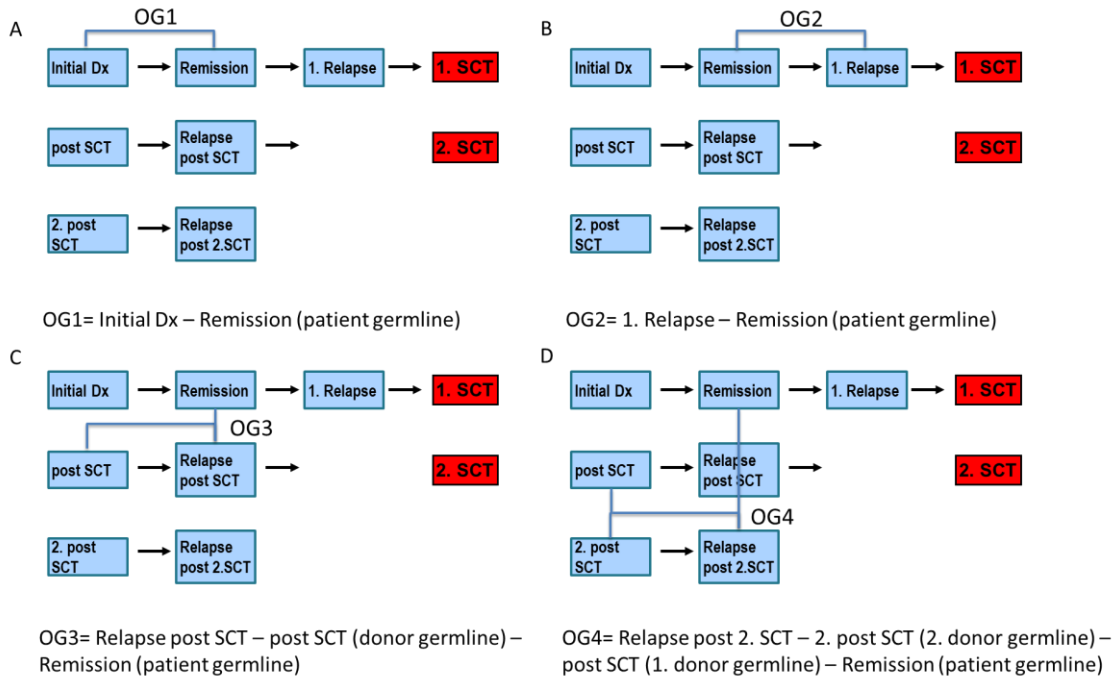

Fig. 6: Calculation of oncogenomes (OGs). A) Calculation of OG1 by subtracting remission sample from initial diagnosis sample. B) Calculation of OG2 by subtracting remission sample from relapse sample. C) Calculation of OG3 by subtracting remission sample and remission post transplantation sample from relapse after first allo-SCT. D) Calculation of OG4 by subtracting remission sample and both remission post transplantation samples from relapse after second allo-SCT. Dx, diagnosis; SCT, stem cell transplantation.

3.3 Calculated oncogenomes are exclusive to patients and disease states

The bioinformatically calculated oncogenomes of the three patients during different steps of the disease (OG1-4) are shown in **Table 13**. It can be seen, that there are large differences in the number of oncogenome sizes, both, at different points in time of the disease and within the patient cohort. The reason for the high number of single nucleotide variants (SNVs) (725) in OG3 of patient 705 likely is explained by mutations in DNA polymerase genes, such as POLG, REV1 and POLM, which subsequently lead to many other mutations, due to failures in DNA synthesis. Patients 202 and 337 do not show mutations in polymerase genes. It can be observed that there is no continuity in the number of mutations during the different stages of the disease. The gene mutations change from stage to stage in the progression of the disease. Also, within the patient cohort there is no consistency in the number of mutations at a particular stage such as the first relapse (OG2). Patient 202 shows 47 SNVs, patient 337 has 34 SNVs and patients 705 has 25 SNVs.

Patient ID	OG1		OG2		OG3		OG4	
	SNVs	Mutated genes	SNVs	Mutated genes	SNVs	Mutated genes	SNVs	Mutated genes
202	N/A	N/A	47	45	57	58	41	41
337	16	16	34	34	62	59	72	69
705	N/A	N/A	25	23	725	624	52	47

Table 13: Calculated oncogenomes in the patients. After bioinformatic processing the numbers of leukemia specific mutations are shown in this table; absolute number of mutations (SNVs) and number of affected genes vary within the patients and the oncogenomes (OGs). N/A: not available

The fact that the mutational spectra vary greatly is again indicated in **Fig. 7**. Shown are the numbers of SNVs and mutated genes in the different stages of the disease (OG1-4). It can be seen, that the number of non-overlapping SNVs

is notably larger than those occurring in all disease stages. Therefore, we conclude that each disease stage should be regarded as a new disease with a new mutational range.

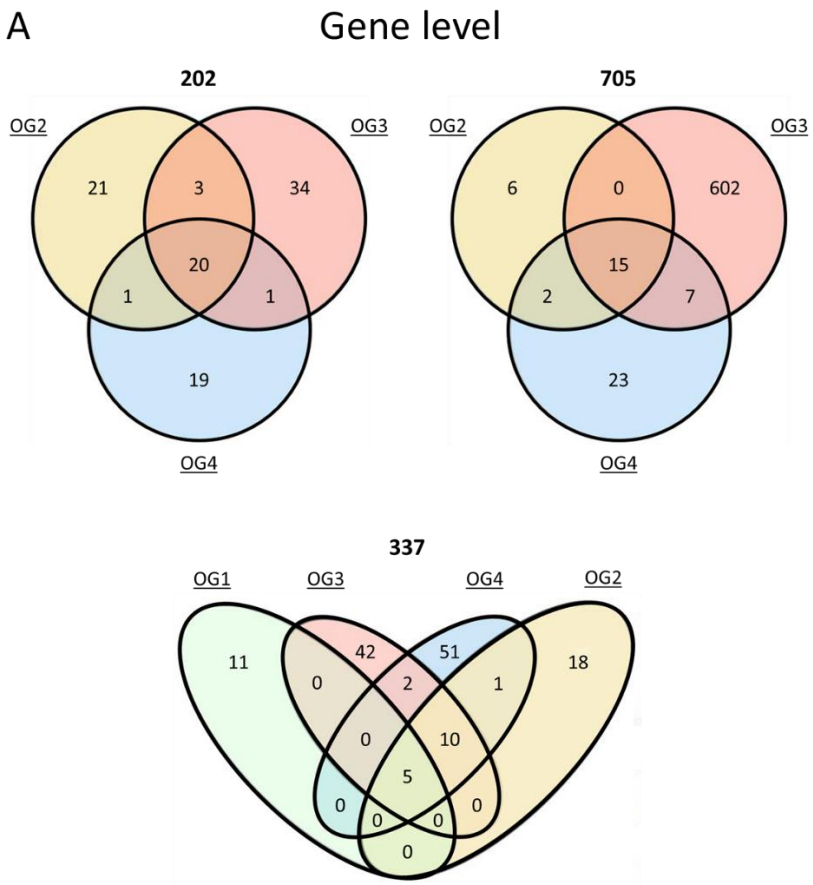

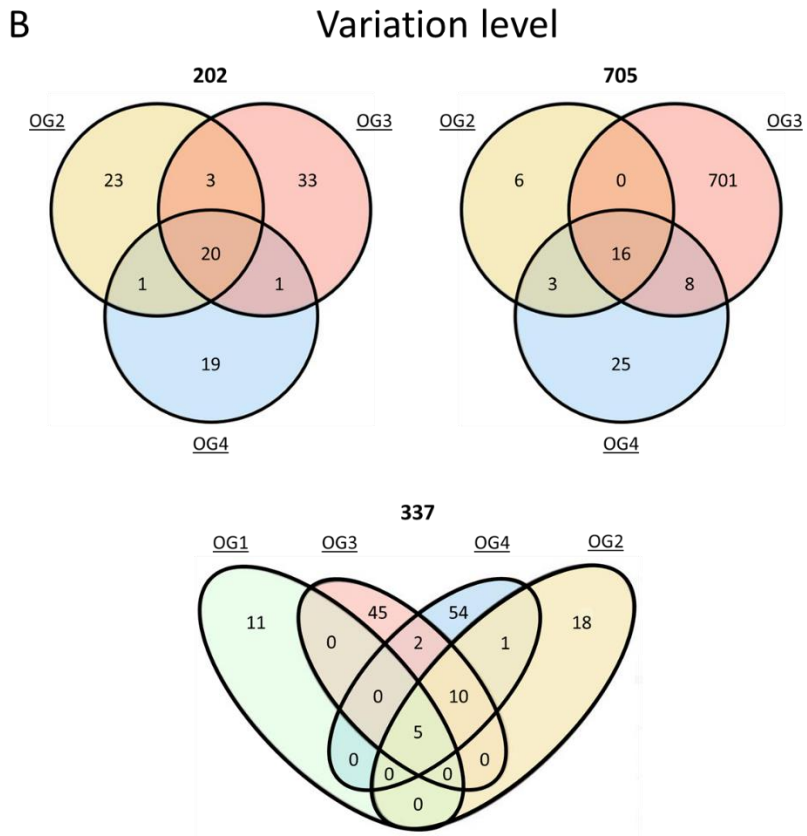

Fig. 7:Mutated gene and SNV level of the different patients. A) Overview of mutational spectra on gene level in the three analyzed patients in OG1, OG2, OG3 and OG4, (OG1 missing in 202, 705). The number of mutated genes in the individual disease stages (OG1-4) is shown. Non-overlapping regions indicate genes specific to the disease stage. Overlapping regions show that the same gene mutations occur in different oncogenomes. B) Overview of mutational spectra on individual variation level. The number of SNVs in the individual oncogenomes is shown. Again, non-overlapping regions are identifying nucleotides mutated in the particular oncogenome. Overlapping regions indicate that the same SNVs occur in different oncogenomes.

3.4 Clonal diversity of each leukemia

In order to reveal the variability of the genetic pattern, we present in **Fig. 8** A-C the genes that were mutated in the relapse after second allo-SCT (OG4). A clear difference can be recognized in the continuous or discontinuous presence of the mutated genes. In addition, the mutated genes also vary within the different oncogenomes of patients 202, 337 and 705.

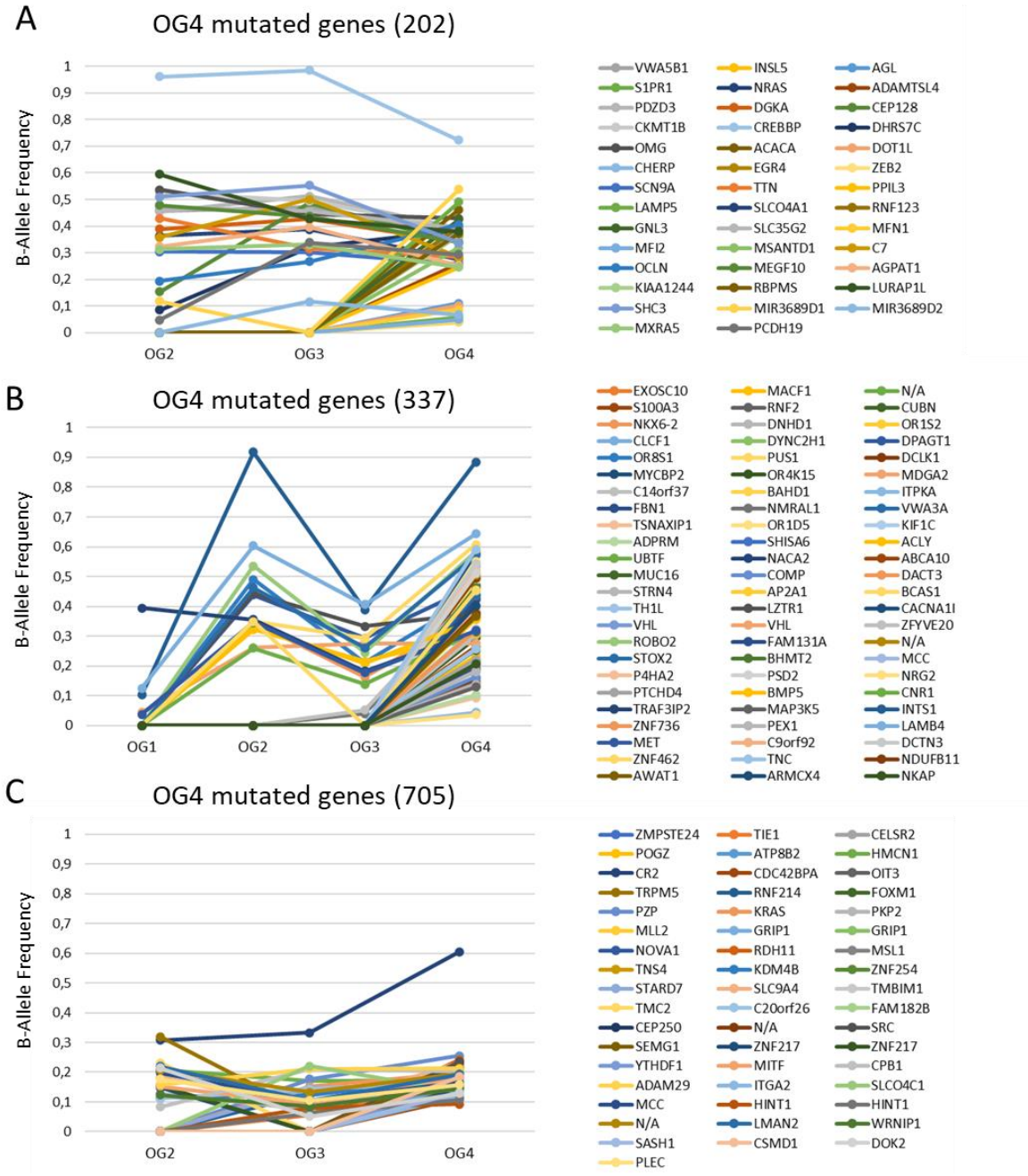

Fig. 8: Mutated genes occurring in oncogenome 4. Each colored line in the diagram represents a different gene that is mutated in OG4. A) Overview of the mutated genes in OG4 including the B-allele frequency of the variant during different steps of the disease (OG2, OG3) in patient number 202. B) Overview of the mutated genes in OG4 including the B-allele frequency of the variant during different steps of the disease (OG1, OG2, OG3) in patient number 337. C) Overview of the mutated genes in OG4 including the B-allele frequency of the variant during different steps of the disease (OG2, OG3) in patient number 705.

In figures 7 and 8 we show the course of individual genes in more detail. **Fig. 9** shows all those genes that are mutated at any time of the disease in the individual leukemias. Again, the number of mutated genes among the patients (5 in 337 and 20 in 202) as well as the genes themselves vary. **Fig. 10** shows all those genes which only occur mutated at the last recurrence of the disease (OG4) and did not occur in the previous disease-stages. Which of these genes are likely more responsible for the aggressiveness of the leukemia will be discussed in the course of this thesis.

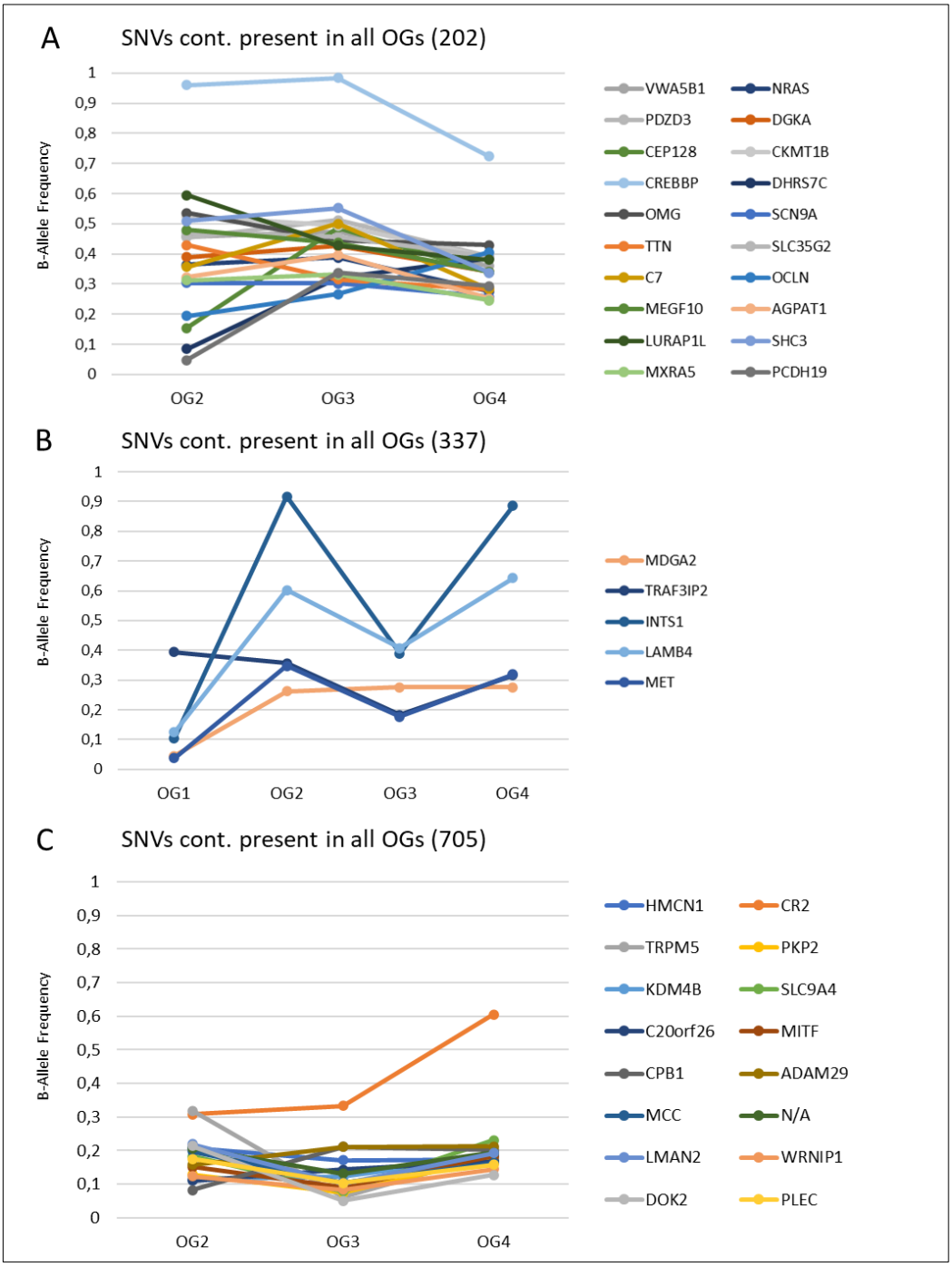

Fig. 9: Continuously present SNVs in all oncogenomes. Each colored line represents a different mutated gene. The variant is continuously present in all oncogenomes, which thus might be responsible for the maintenance of the disease. A) Continuously present SNVs in patient 202. B) Continuously present SNVs in patient 337. C) Continuously present SNVs in patient 705. Cont.: Continuously.

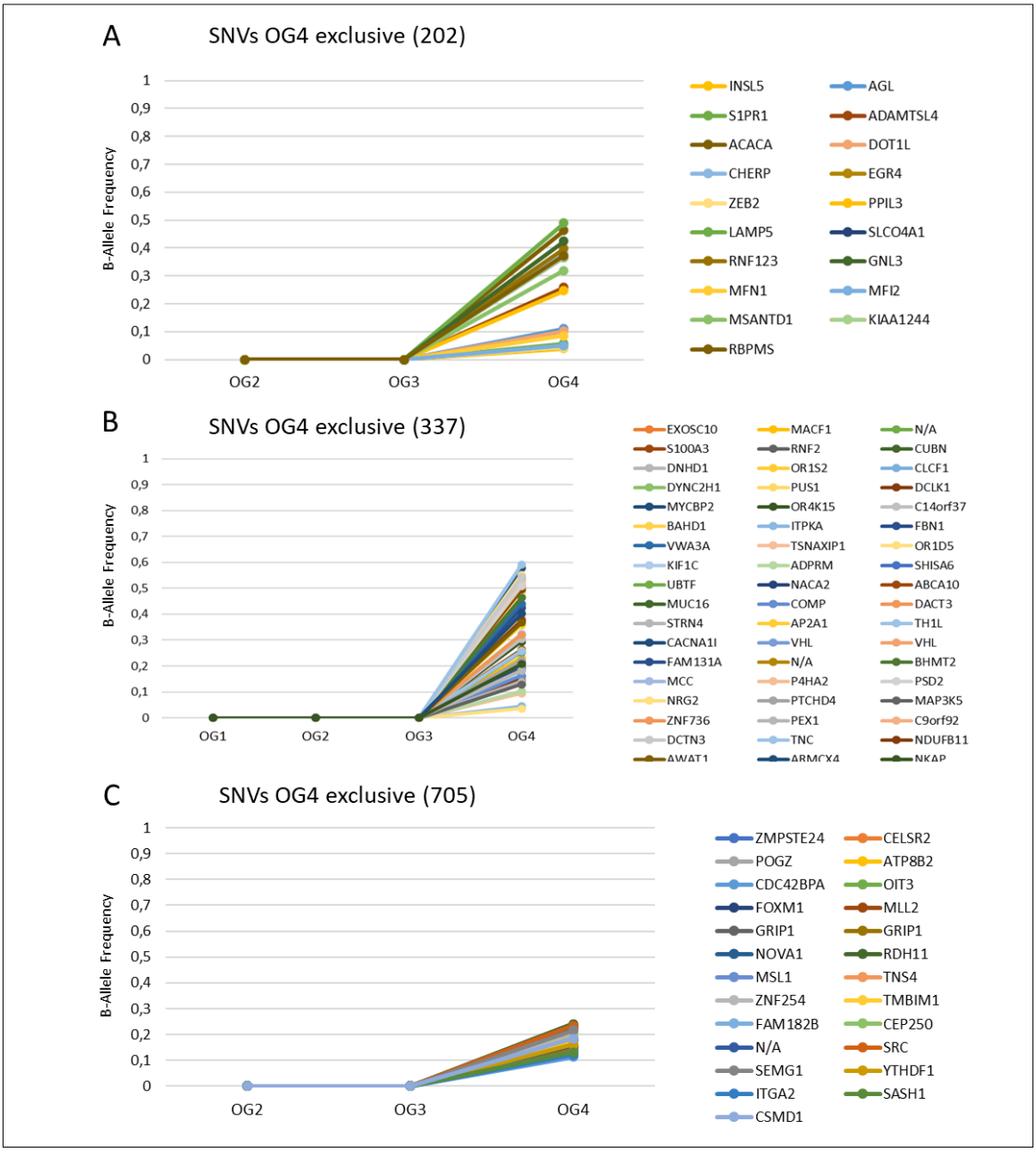

Fig. 10: Oncogenome 4 exclusive SNVs. SNVs that are exclusively present in OG4, which might have driven the last relapse after second allo-SCT. A) Exclusive SNVs in OG4 of patient 202. B) Exclusive SNVs in OG4 of patient 337. C) Exclusive SNVs in OG4 of patient 705.

3.5 Genes of interest

In the following, we analyzed, which cancer-relevant genes were mutated in the different leukemias/relapses. Variants in these genes, classified as cancer genes by the cancer gene census, were found in all our patients. Mutated genes included NRAS, CREBB, MET, VHL, KRAS, MLL2 and MITF. We also identified

genes in all patients in the final relapses that could be targeted by novel therapeutic agents. These included NRAS, DOT1L, NRG2, MET, KRAS and SRC. Thus, all patients in the relapse after second allogenic stem cell transplantation had aberrations in genes that are both considered cancer-relevant and potentially treatable, so that these genes could be considered in the choice of therapy. Our findings regarding the high plasticity of patient-specific oncogenomes over time and the great diversity between patients underline the urgent need to analyze the oncogenome of each leukemia. The SNVs that are potentially targetable are subject to change from relapse to relapse and vary widely from patient to patient. Genes of interest are shown in **Fig. 11**.

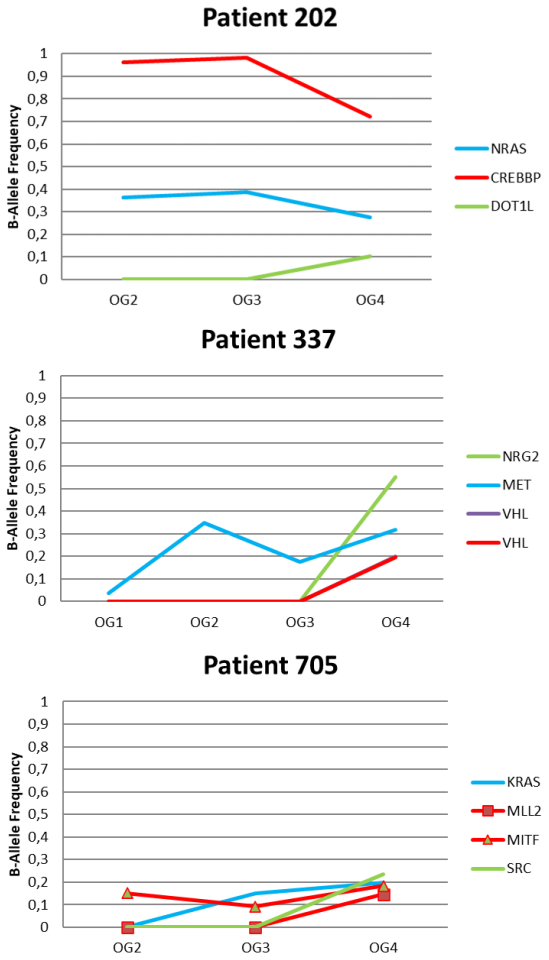

Fig. 11: Mutated druggable and CGC-genes. Red lines represent mutated genes in the patients, that are listed as cancer genes in the cancer gene census (CGC); green lines mark genes that can be used for targeted therapy; blue lines outline those genes that are both, in the CGC and druggable.

3.6 Druggable targets even in the last relapse

In post allo SCT-relapse, mutated genes exist in every patient, which can be targeted by specific therapy. In patient 202 NRAS is druggable and described as cancer gene, in patient 337 it is the MET gene and in patient 705 KRAS. For NRAS and KRAS mutations drugs indirectly targeting the RAS/RAF/MEK/ERK pathway (also known as MAPK pathway) are available such as the MEK-inhibitors trametinib and selumetinib. There are currently two studies investigating these tyrosine kinase inhibitors in pediatric leukemia (NCT03190915, NCT03705507). MET mutations can be directly targeted by tyrosine kinase inhibitors such as cabozantinib or crizotinib. The latter is currently evaluated in a phase II trial in children with acute myeloic leukemia (NCT02638428). Mutated genes and potential corresponding therapies are shown in **Table 14**.

	Druggable Gene	Directly druggable gene (family)/pathway	Indirectly actionable gene (family)/pathway	Approved drug available	Approved drugs (not restricted to EU-approval)	Ongoing clinical trial and National Clinal Trial (NCT) number
202	NRAS	NRAS	MEK, (RAF, ERK, PI3K, AKT, MTOR)	Y2	Trametinib, selumetinib (MEK-Inhibitors)	Phase II trial of trametinib in children with r/r juvenile myelomonocytic leukemia (JMML), (NCT03190915); Phase I/II trial of selumetinib in children with r/r RAS pathway mutated ALL (NCT03705507)
337	MET	MET	MEK, PI3K, AKT, MOTR, (RAF, ERK)	Y1	Cabozantinib, crizotinib	Phase II trial of, inter alia, crizotinib in children with r/r solid tumor and AML (NCT02638428); In vitro sensitivity directed chemotherapy in patient with relapsed or refractory acute leukemia (NCT02551718)
705	KRAS	KRAS	MEK, (RAF, ERK, PI3K, AKT, MTOR)	Y2	Trametinib, selumetinib (MEK-Inhibitors)	see NRAS

Table 14: Druggable genes found in the patients. Y1: Yes, as a direct drug target; Y2: Yes, as an indirect drug target; r/r: relapsed and refractory; ALL: Acute lymphoblastic leukemia; AML: Acute myeloid leukemia

3.7 Validation by Sanger sequencing

The actual presence of the SNVs still needed to be validated by Sanger sequencing. The SNVs to be validated were derived from Fig. 11 as they were either classified as cancer genes or were potentially targetable. To validate the

SNVs of genes of interest, PCRs were performed from the relapse post second allo-SCT samples and then confirmed by Sanger sequencing. This was successful for all the above-mentioned genes and results are shown in **Fig. 12**.

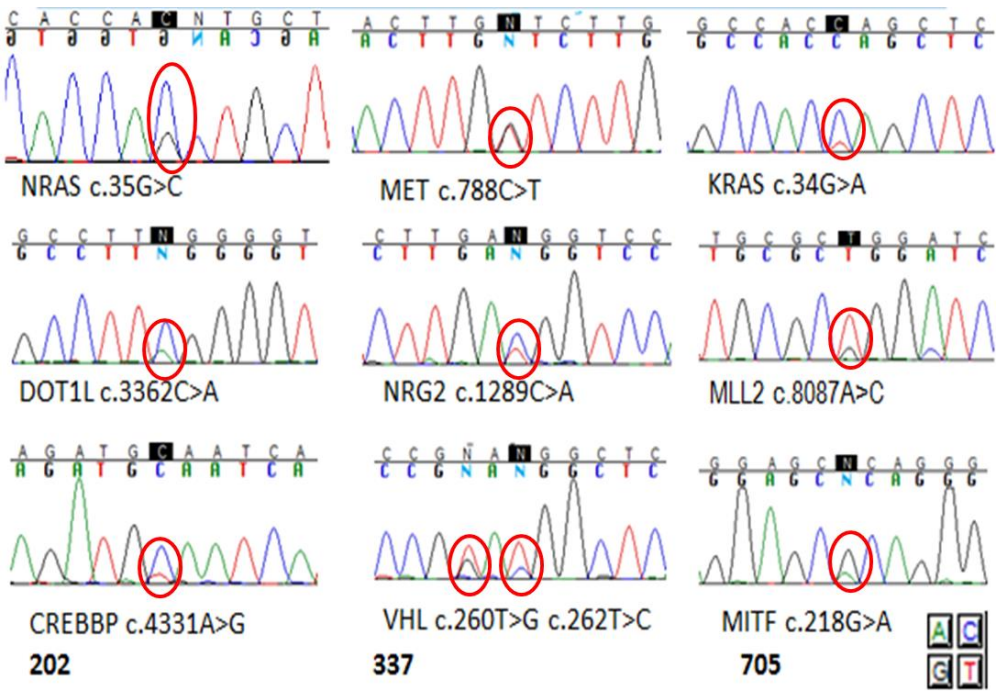

Fig. 12: SNVs validated by Sanger sequencing. SNVs of genes of interest were validated by Sanger sequencing from the relapse post second allo-SCT samples. Figure shows location and change of bases of the mutated genes. Green peaks represent adenosine; blue peaks represent cytosine; black peaks represent guanine; red peaks represent thymine. Mutations are indicated for each patient and highlighted with red circles.

3.8 Preparation of functional analysis and cloning strategy

The next step was to functionally test the mutated genes. We knew that they represented cancer genes and that they could be targeted therapeutically. However, we also wanted to find out, whether the mutations of our patients would cause e.g. proliferative behavior in BA/F3 cells. BA/F3 cells are murine pre-B cells that can grow in an IL3 factor-dependent manner [48]. If a mutation occurs downstream of IL3 in the signaling pathway, it can lead to IL3-independent proliferation. To later enable functional analysis, we prepared BA/F 3 cells as described below (**Fig. 13**).

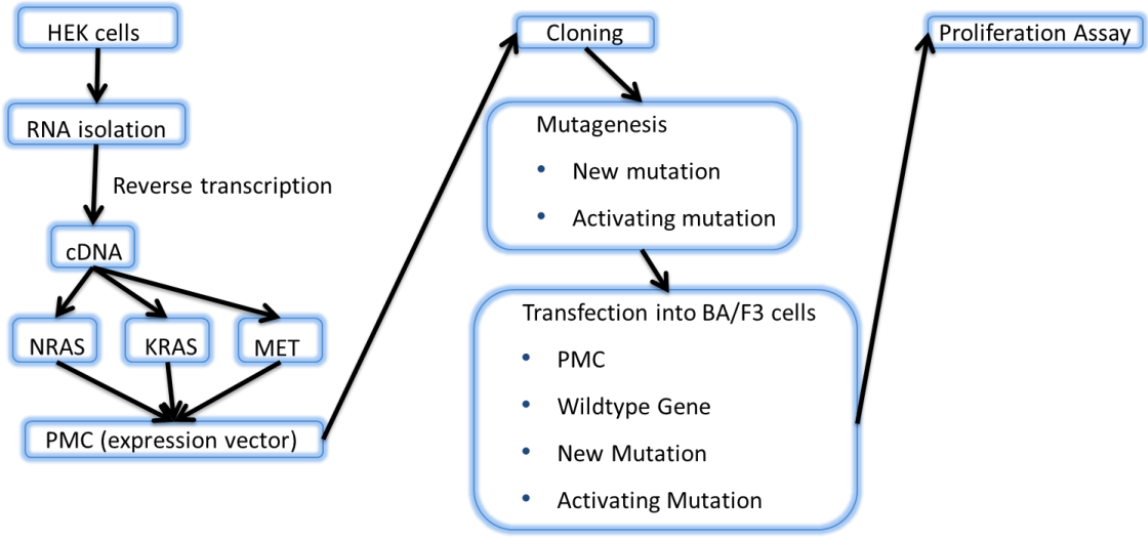

Fig. 13: Cloning strategy. Cloning of mutated NRAS, KRAS and MET into expression vectors, that are later transfected into BA/F3 cells; steps: isolation of RNA from HEK cells, transcription into cDNA, ligation into PMC expression vector, cloning of the vector in E. coli, mutagenesis of patient's mutation and activating mutation, transfection into BA/F3 cells including the transfection of two negative controls (empty vector and vector with wildtype gene), proliferation assay with transfected cells.

3.8.1 Isolation of NRAS, KRAS and MET from cDNA

After isolating RNA from HEK cells, we transcribed it by reverse transcription into coding DNA (cDNA). From cDNA we isolated the coding regions of the genes of interest NRAS, KRAS and MET. The coding regions from NRAS, KRAS and MET are shown in **Fig. 14**. NRAS is 583 base pairs (bp) long with its gene length of 570 bp and the primer designed for restriction. KRAS has the same length. MET is significantly longer with a total length of 4250 bp.

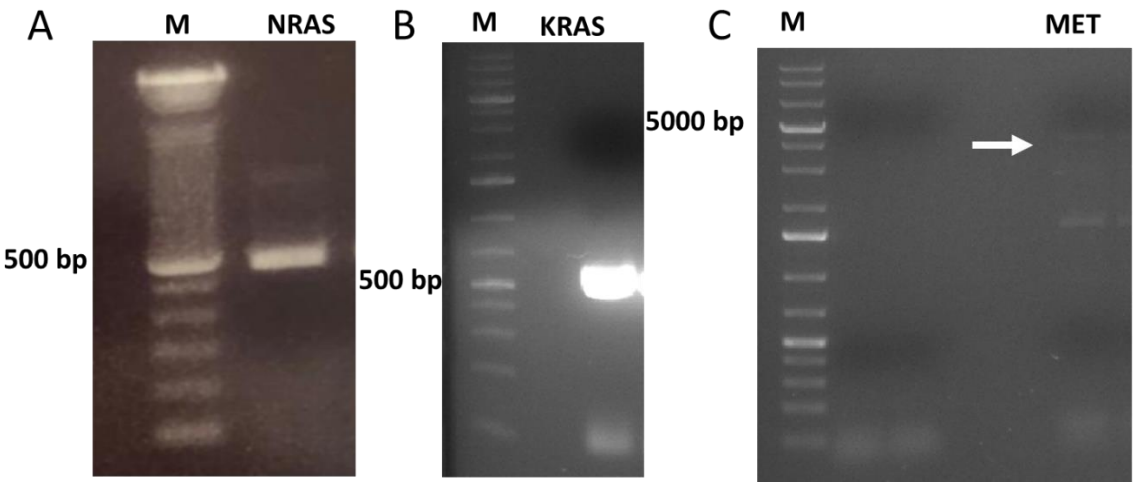

Fig. 14: Coding regions of NRAS, KRAS and MET isolated from cDNA. A) Presentation of NRAS in 1% agarose gel. M: Marker, Gene Ruler 100 bp ladder (Invitrogen). NRAS is found at the correct size according to its length. B) Presentation of KRAS in 1% agarose gel. M: Marker, Gene Ruler 1 Kb Plus ladder (Thermo Scientific). KRAS is found at the correct size according to its length. C) Presentation of MET in 1% agarose gel. M: Marker, Gene Ruler 1 Kb Plus ladder (Thermo Scientific). MET is found at the correct size according to its length.

3.8.2 Restriction digestion

The insertion of the coding regions into the transfection vector required the use of restriction enzymes. For NRAS and KRAS we used MluI and SalI. For MET we used MluI and HindIII (**Fig. 15**).

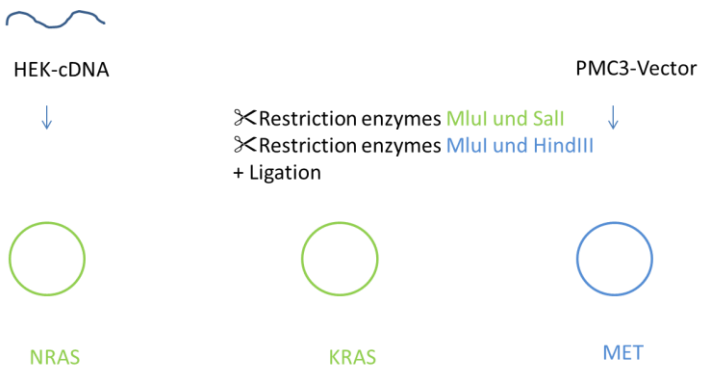

Fig. 15: Restriction enzymes used for cloning. HEK-cDNA and PMC3-expression vector were cut with restriction enzymes to ligate them again to form the transfection vector including the necessary gene. For NRAS and KRAS MluI and SalI were used and for MET we used MluI and HINDIII.

To assess correct cloning, we performed a restriction digest. By separation of the reaction products on a gel we could see, if the cut vector and gene were running at the right level and therefore were cloned correctly (**Fig. 16**). If the plasmid had not been cut at all, it separated in the gel according to **Fig. 16 A**, as it is visible in a circular and supercoiled form.

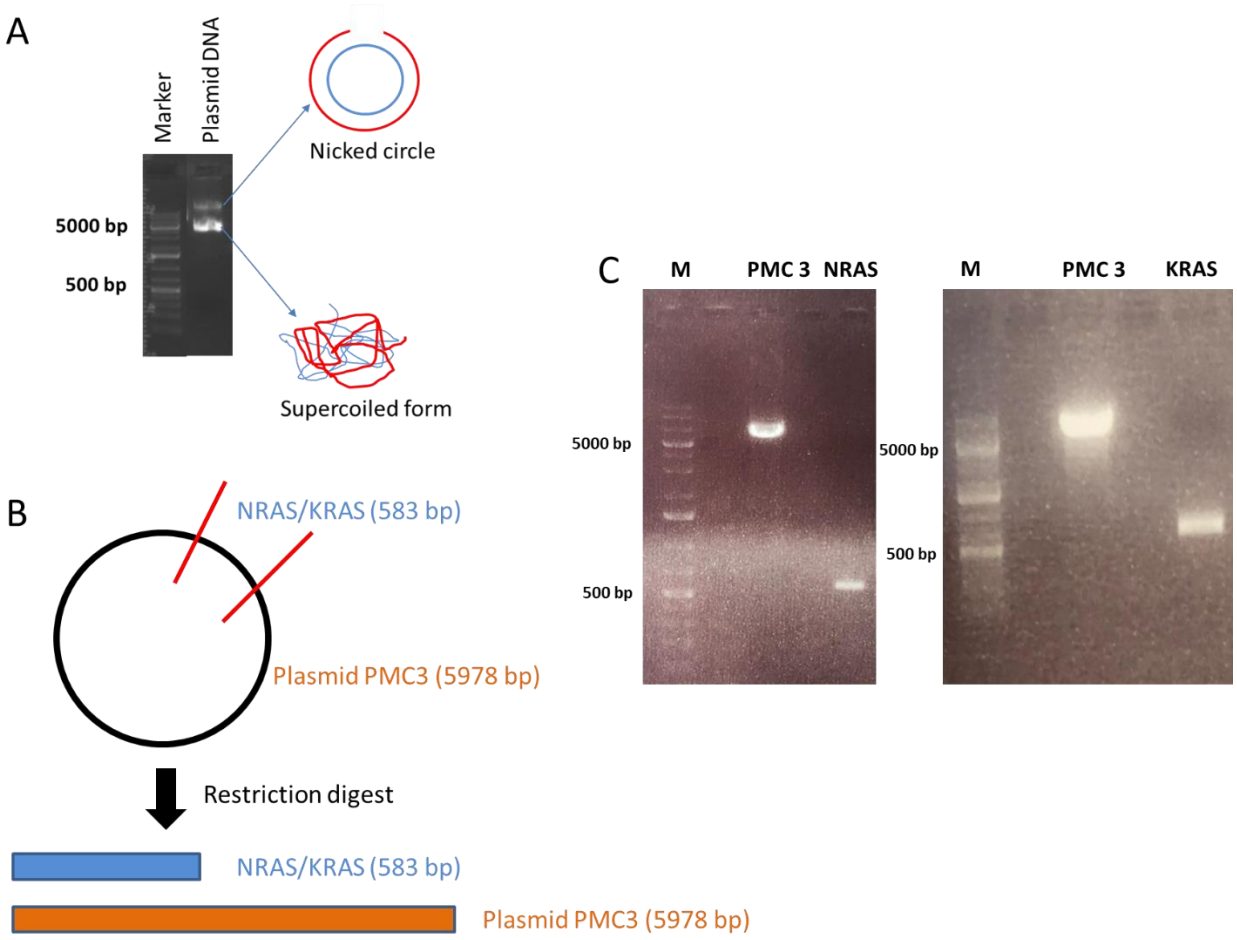

Fig. 16: Restriction control for NRAS and KRAS. A) Presentation of an uncut plasmid**:** an uncut plasmid typically exists in two forms – in circular and in supercoiled form. Therefore, it is separated to different heights when run on a gel. The circular form is difficult to shape and runs further up in the gel, while the supercoiled form is more compact an can thus penetrate through the meshes of the gel so that it runs further down in the gel. B) A schematic example of the control of the restriction digestion of NRAS and KRAS with its plasmid is shown here. NRAS and KRAS are 583 base pairs (bp) long after digestion with MluI and SalI. The plasmid PMC3 is 5978 base pairs long after restriction digestion. C) Presentation of NRAS and PMC3 and KRAS and PMC 3 after restriction in 1% agarose gel. M: Marker, Gene Ruler 1 Kb Plus ladder (Thermo Scientific). PMC3 and NRAS/KRAS are to be found at the correct size according to their length. MET data is not shown in this figure.

To check, whether the gene was inserted into the plasmid without addition of novel mutations, we performed Sanger sequencing after cloning of the new gene containing vector. These showed a mutation-free incorporation of all three genes into the plasmid.

3.8.3 Mutagenesis

To introduce our mutations as well as the previously described activating mutations into the transfection vector we designed primers containing the desired mutations. After mutagenesis according to the Q5® Site-Directed Mutagenesis Kit, we used Sanger sequencing to check for the success of the mutagenesis. The mutations we introduced are shown in **Table 15**. The vectors were now cloned as desired and are ready to be further evaluated in later work.

Gen		Substitution on cDNA level	Substitution on protein level
NRAS	Patient‘s mutation	c.35G>C	G12A
	Activating mutation	c.35G>A	G12D
KRAS	Patient‘s mutation	c.34G>A	G12S
	Activating mutation	c.35G>T	G12V
MET	Patient‘s mutation	c.788C>T	T263M
	Activating mutation	c.3803T>C	M1268T
	Activating mutation tested on BA/F3 cells	c.3029C>T	T1010I

Table 15: Mutations inserted by mutagenesis. Mutagenesis was used to insert the above-mentioned mutations into the three CDS-containing (CDS: Coding Sequence) plasmids. Shown is the point mutation on cDNA level and the modified protein. G: guanine, C: cytosine, A: adenine, T: thymine. The letters of the proteins correspond to the 1-letter code according to IUBMB (International Union of Biochemistry and Molecular Biology).

3.9 Clinical case of medulloblastoma-patient co-occurring with café-au-lait spots

The following paragraphs were published in Chiu et al., 2019 [1]

Our patient was diagnosed with a medulloblastoma at the age of 3 years, when he presented to a local hospital with vomiting, vertigo and headache for several days in addition to an increased tendency to fall. A cranial MRI scan showed a large infratentorial tumor (**Fig. 17 A**). The patient was then transferred to our tertiary care hospital for subsequent diagnosis and therapy. On admission, his general state of health was reduced, and the neurological examination showed a broad-based gait. Additionally, multiple café-au-lait spots and inguinal freckling were noted. The parents reported, that they themselves as well as their three children had the same skin lesions (**Fig. 4**; the youngest child had not been born at the time) and that a neurofibromatosis type 1 work-up had previously been performed but had been negative.

After excision, the tumor was histologically classified as a desmoplastic medulloblastoma WHO grade 4, SHH-activated. Tumor material was first analyzed via next panel sequencing for SNVs in genes commonly mutated in medulloblastoma (CTNNB1, APC, SMO, SUFU, PTCH1, FBXW7, TP53, DDX3X, KMT2D, TERT promotor). Except for a heterozygous DDX3X SNV all other genes showed wildtype sequences.

The postoperative MRI showed that a total resection had been achieved, however, tumor cells were found in CSF (M1). Adjuvant chemotherapy according to the HIT 2000 Interim Register (therapy group A.6.) was administered over 10 months and consisted of five cycles comprising vincristine, cyclophosphamide, carboplatin, VP16 and high-dose methotrexate plus intra-ventricular methotrexate.

Shortly after the end of the last chemotherapy cycle the patient again started to vomit and additionally complained about back pain. The MRI scan now showed a relapse of the hyperintense infratentorial tumor and new diffuse intraspinal metastases (**Fig. 17 B**). Medulloblastoma cells were again found in the CSF, thus

confirming the diagnosis of disseminated relapse. After interdisciplinary discussions and several conversations with the parents, it was decided to discontinue curative and to initiate palliative therapy. The patient only survived relapse diagnosis for four weeks. Several years after our index patient had passed away, his youngest brother was diagnosed with T-lymphoblastic lymphoma at the age of three years. In this case, the family refused genetic testing.

Due to the consanguinity of the parents and the unusual combination of a highly aggressive cancer and concomitant skin alterations, the suspicion of a genetic (most likely autosomal-recessive) cancer predisposition was raised. As the patient received four points (thus making him eligible for testing) on the diagnostic scale suggested by the European consortium ‘Care for CMMRD’, CMMRD also had to be excluded in our index patient.

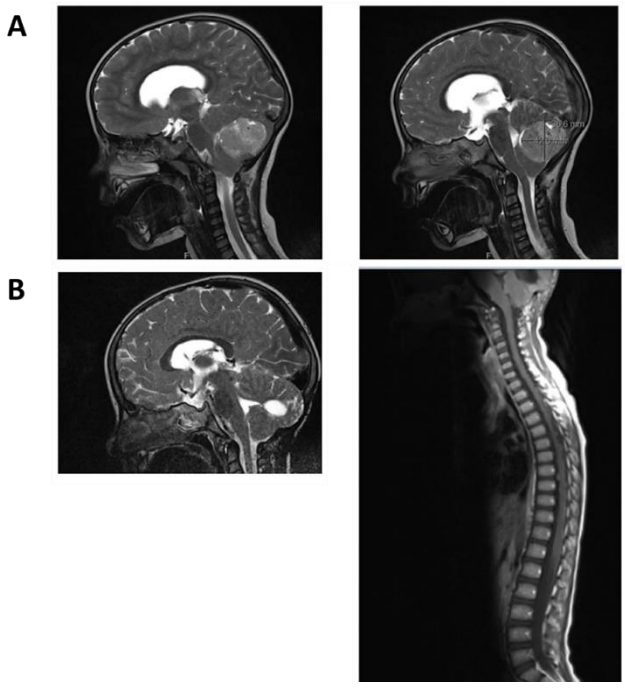

Fig. 17: MRI-scan of the index patient. A) Sagittal T2-weighted cMRI demonstrating the infratentorial preoperative medulloblastoma. B) Sagittal T2-weighted cMRI showing the relapsing infratentorial medulloblastoma and sagittal T1-weighted spinal MRI showing intraspinal metastases. Reproduced from Chiu et al., 2019 [1].

3.10 Performing WES in the medulloblastoma patient to identify germline SNVs

The following paragraphs were published in Chiu et al., 2019 [1]

We performed WES of our index patient as well as of his parents and siblings, as they also exhibited the skin lesions described above but had not received a cancer diagnosis up to the time of our analysis.

To only identify relevant SNVs, we defined the following inclusion criteria: (1) only mutations occurring with GMAF below 1%, (2) all those SNVs, which were homozygous in our index patient and heterozygous in both parents and the siblings (as all of them had the skin alterations but were tumor-free at least until the moment of testing), (3) annotated genes with non-synonymous coding changes, (4) both prediction tools SIFT and Polyphen had to predict a change deleterious to protein function. Highly polymorphic regions were excluded. Employing these criteria, we received three potentially disease-causing SNVs, namely in the genes guanidinoacetate N-methyltransferase (GAMT), primary cilia formation (PIFO) and SON DNA-binding protein (SON) (**Table 16**).

GAMT was mutated in c.79T > C, which changes tyrosine to histidine (Y27H). This alteration was described previously as a variant without an effect on protein activity [49]. PIFO presented with a single nucleotide variant on position c.239G > A changing arginine to lysine (R80K). This SNV was previously identified in patients with severe ciliopathies such as left–right asymmetry, polycystic kidney disease (PKD) or double outlet right ventricle (DORV) as PIFO regulates primary cilia disassembly [50]. As our patient had no clinical signs of a ciliopathy, we did not further take this gene into consideration and focused on the third candidate instead. However, it must be noted that ciliopathies are highly pleiotropic diseases with varying degrees of penetrance within any given tissue as well as between patients [51]. Additionally, a compartmentalization of Hedgehog signaling at primary cilia in medulloblastoma was recently reported, which is also of therapeutic interest [52].

Chr	Position	Ref	Alt	Ensembl gene ID	Gene	gMAF	Amino acid substitution
19	1401397	A	G	ENSG00000130005	GAMT	<0.01	Y/H
1	111890375	G	A	ENSG00000173947	PIFO	<0.01	R/K
21	34923207	C	T	ENSG00000159140	SON	<0.01	A/V

Table 16: Identified homozygous SNVs. Affected chromosomes, altered position, reference genome, alterations, gene names and GMAF are indicated. Polyphen and SIFT predicted the SNVs as deleterious/probably damaging for protein function. Chr: Chromosome, ref: reference, alt: alteration, GMAF: general minor allele frequency. Modified from Chiu et al., 2019 [1].

Our patient carried a point mutation (c.1670C > T) in *SON*, which altered the alanine in position 557 to valine (A557V). Conventional Sanger sequencing confirmed the presence of this SNV (**Fig. 18**).

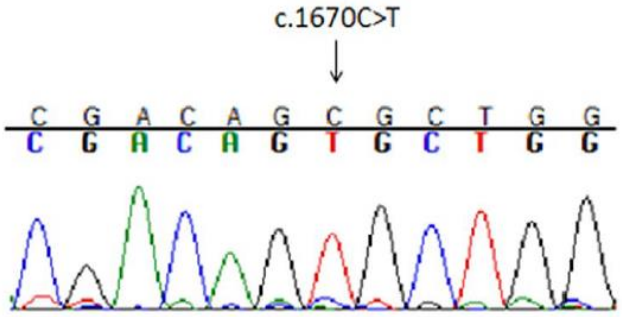

Fig. 18: SNV validation. Confirmation of the homozygous mutation of SON in the index patient by Sanger sequencing. Reproduced from Chiu et al., 2019 [1]

3.11 Exclusion of other potentially alterated genes

The following paragraphs were published in Chiu et al., 2019 [1]

The most frequent differential diagnoses for café-au-lait spots include neurofibromatosis, McCune-Albright syndrome, tuberous sclerosis, and Fanconi anemia. To exclude the genes commonly mutated in those diseases we specifically (in addition to our previously described whole-exome approach) investigated the frequency of alterations in the following genes: NF1, NF2, GNAS1, TSC1 and TSC2, BACH1(FANCJ/BRIP1), FANCA. Also, we

investigated genes associated with hereditary medulloblastoma (APC, BRCA2, CREBBP, EP300, POLE, PTCH1, SMO, TP53).

Additionally, we searched for mutations in any of the genes causing constitutional mismatch repair deficiency syndrome (CMMRD) as well as in SUFU, which predisposes to medulloblastoma. Intronic mutations, those with GMAF > 1% and those not occurring in all family members were excluded. We did not detect any SNV in any of these genes fulfilling these criteria. When considering all genes, we did not detect any SNV, which was homozygous in our index patient and not present in other family members. Looking at SNVs, which were heterozygous in the index patient and not present in other family members only three SNVs were identified, namely in ALG3, in which defects have been associated with congenital disorder of glycosylation type Id (CDG-Id); CHD3, a component of the histone deacetylase complex Mi-2/NuRD complex; PABPC3, a poly(A)-binding protein with functions in translation initiation.

4 Discussion

4.1 Small patient cohort and importance of genetic mutation analysis

Acute lymphatic leukemia is the most common childhood tumor entity, accounting for 30% of all pediatric tumors. It has an overall good prognosis of about 90% survival rate [8, 53]. Unfortunately, relapses and aggressive courses of the disease occur, which are not yet fundamentally understood on a genetic level. Currently, there are no standard therapies available for a subset of these patients. The cohort of patients with multiple relapses despite stem cell transplantation is very small, which is why large treatment study for these patients are not available. We analyzed the leukemic exomes of three patients who underwent two stem cell transplantations and thus a total of three relapses after initial diagnosis. Even though these are rare cases, the importance of understanding such an aggressive disease should not be underestimated. Only if a gene-wide analysis with WES is performed at the time of relapse and the corresponding driver mutations are detected, the patients can be further treated in a timely manner. Instead of standardized therapy protocols, an individualized therapy approach must then be chosen for these rare cases.

4.2 High diversity between the patient cohort and between each step of the disease

ALL is defined as a disease with either chromosomal translocations, or specific somatic aberrations resulting in a large variety of subgroups. It thus represents a very heterogeneous disease, which we could also observe in our cohort [54, 55]. After analyzing pediatric ALL patients with multiple relapses after two SCTs, we observed no overlapping mutations within our patient cohort of three patients. This leads to the realization that every patient must be treated individually at every stage of the disease.

Due to clonal evolution of leukemic blasts, mutations occurring during the initial disease are not obligatory present in the subsequent or any of the relapses. New

leukemic subclones can arise by obtaining new mutations. By proliferation of a new clone with different mutations the relapse is a new disease. This is shown by the fact that, on the one hand, the number of mutations varies greatly from patient to patient (for example 25 mutations in OG2 of patient 705 and 703 mutations in OG3) and on the other hand the affected genes vary to a large extent. This means that each stage of the disease has a unique mutation profile which is responsible for the disease.

4.3 Patterns of mutational spectra

Interestingly, we were able to identify patterns within the mutation spectra. There were such genes that were continuously mutated through all stages of the disease. It could be assumed that these genes are responsible for the latent maintenance of the disease, as they can be found in every disease stage. For example, NRAS was able to assert itself as an oncogene again and again. Furthermore, there were genes that could only be found in oncogenome 4. These could be the reason for the aggressiveness and the development of the last relapse. Due to a selective pressure on the blast cells to survive, the mutational spectrum can change significantly in each relapse of the disease.

4.4 Druggable cancer genes in the last relapse

Even though leukemic disease was already advanced in our patient cohort, we were able to identify mutated cancer genes in the relapse after second stem cell transplantation, which can be targeted therapeutically. In patient 202 we identified NRAS, patient 705 KRAS and patient 337 MET. All found Mutations were described previously as pathogenic since they are located in hotspot regions [56]. However, these mutations should be investigated further because it is not yet possible to say, whether these SNVs really are the main driver mutations or whether it is the combination of several gene mutations that is responsible for relapse. Further functional and preclinical studies are necessary in this context to confirm the consequences of the identified gene mutations and their influence on therapy.

Our analysis provides so far the first comprehensive genetic characterization of pediatric ALL relapses after second allo-SCT. Basically, it is possible to identify treatable targets in the relapses, which makes personalized analyses and the resulting therapies important. Our finding of all three patients with genetic lesions in druggable genes could have essential clinical implications as it opens the way for the elucidation of new therapeutic targets in multi-relapsed ALL patients.

4.4.1 NRAS and KRAS

NRAS (Neuroblastoma Rat Sarcoma) and KRAS (Kirsten Rat Sarcoma) are part of the RAS gene family and belong to the small GTPase superfamily. They act as central elements in a number of signal transduction pathways. Those pathways are involved in the regulation of cell growth and differentiation. NRAS and KRAS proto-oncogenes are monomeric G protein consisting of 189 amino acids. A single amino acid substitution is responsible for an activating mutation turning them into tumor driving genes. The resulting transformed KRAS protein is involved in several malignant tumors, including lung adenocarcinoma [57], ductal carcinoma of the pancreas [58, 59] and colorectal carcinoma [60]. Mutated NRAS protein has been associated with rectal cancer [61] and follicular thyroid cancer [62]. In addition, NRAS and KRAS mutations have been reported in several leukemia subtypes [63-66]. Their direct involvement in the development of many tumors makes NRAS and KRAS attractive targets for novel cancer drugs, such as deltarasin [67], a direct KRAS inhibitor, or trametinib, a direct MEK inhibitor and additionally an indirect KRAS/NRAS inhibitor [68]. Also in a recent study selumetinib was investigated as a MEK-inhibitor targeting RAS pathway mutations in pediatric ALL [69].

4.4.2 MET

MET proto-oncogene (mesenchymal-epithelial transition factor) encodes a member of the transmembrane receptor tyrosine kinase protein family. The pre-protein is processed proteolytically to produce alpha and beta subunits. Those are linked together by disulfide bonds to form the mature receptor. Binding of its ligand, the hepatocyte growth factor, induces dimerization of two MET-receptors and the phosphorylation of specific tyrosine residues in the C-terminal

intracellular domain and thus activates the receptor. This activation plays a crucial role in various signaling transduction pathways, including MAP cascades, the PI3K-Akt signaling pathway, the JAK-STAT signaling pathway and the activation of the transcription factor NFκB. Activation of MET leads to cellular survival, cellular migration and invasion [70]. Mutations in this gene are associated with multiple cancers [71] including papillary renal cell carcinoma [72], hepatocellular carcinoma [73] and pulmonary carcinoma [74, 75]. Therefore, MET represents an important structure of targeted therapies, such as the use of Tivanitinib or Onartuzumab in lung cancer [76]. MET mutations and other RAS/RTK pathway mutations predominantly STK 11, KIT, NRAS, KRAS, PTEN have also been described in leukemias [77].

4.5 Cloning of genes and mutagenesis – outlook: proliferation assay

Since RAS in its two subforms NRAS and KRAS is mutated in our patients 202 and 705 in their last relapse and are additionally listed among the therapeutically targetable molecules, we hypothesized that it would be useful to test their mutated form for transforming properties.

In the IL3 signaling pathway, RAS is located as a small GTPase downstream of IL3 (**Fig. 19**). BA/F3 cells are murine pre-B cells that grow and proliferate dependent on IL3. The idea is to test, whether the mutations we have found in our patients cause activation of the protein in leukemic cells. If this is the case, BA/F3 cells can grow independently from IL3. For this purpose, the genes to be investigated, NRAS, KRAS and MET, were inserted into the transfection vector PMC3 and the genes were mutated at the corresponding sites as in our patients. The aim of future experiments is to check by performing proliferation assays whether the new mutation can cause an uncontrolled IL3 independent proliferation in a leukemic model just like the mutations described as activating in the literature (NRAS G12D [78], KRAS G12V [79, 80], MET M1268T [81] and MET T1010I [82, 83]. The experimental setup for future projects is shown in **Fig. 20**. The plasmids already cloned in this thesis are going to be transfected in BA/F3 cells. These include the empty vector, the vector with wild-type gene, the

vector with mutated gene and the vector with definitely activating mutated gene. The mutations found in our patients is predicted to lead to growth since they are all located in hotspot locations.

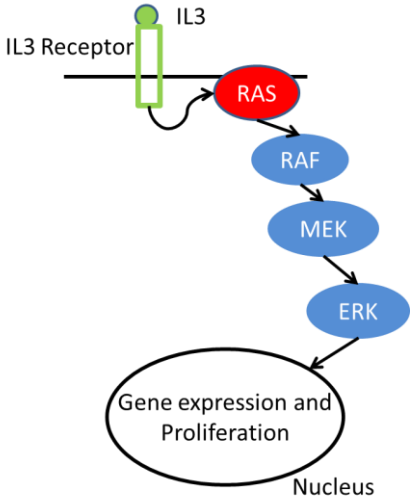

Fig. 19: IL3 Signaling pathway. IL3 binds to the IL3-Receptor. Downstream of the IL3-Receptor is the RAS oncogene, which was mutated in two of our patients. RAS is a small GTPase and has been described as driver gene of different tumors including leukemia. It leads to proliferation of cells when activated.

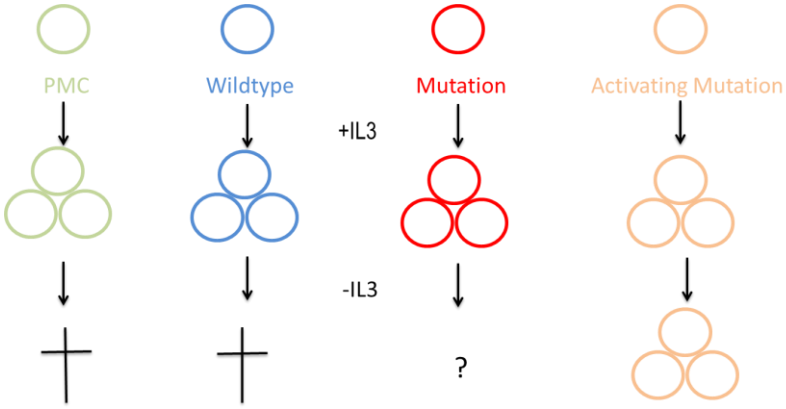

Fig. 20: Aim of proliferation assay. Four vectors are transfected into BA/F3 cells. The empty vector and a wildtype gene as negative controls, a known activating mutation as positive control and the mutation of one of our patients (202: NRAS c.35G>C, 705: KRAS c.34G>A, 337: MET c.788 C>T). First, IL3 is added so that all the cells can proliferate. After IL3 depletion, the negative controls should die, while cells containing the activating mutations still proliferate.

4.6 Limitations of our findings

Overall, an approach to analyze patients with very advanced acute lymphocytic leukemia on a genetic level was developed. However, the number of analyzed patients is still small. Thus, a multi-center study with the goal of examining a larger number of patients in this stage of the disease would be highly desirable. It might be possible to see parallels within the cohort or similarities in the mutated genes. Besides the number of patients, the exclusive performance of WES is also a limiting factor. In addition, amplicon sequencing should be performed for selected SNVs in order to allow a deeper reading of the mutations. The urgent need of functional assays is already mentioned above. In order to analyze the somatic tumor mutations more rapidly, our work also shows, that it should be sufficient to sequence only the current tumor stage, as the tumors differ greatly in their mutation spectrum anyway. This saves time and is already being done in projects like INFORM (INdividualized Therapy FOr Relapsed Malignancies in Childhood) [84].

4.7 A previously not reported point mutation in SON was likely causative

The following paragraphs were published in Chiu et al., 2019 [1]

As mentioned above, our medulloblastoma patient carried a point mutation (c.1670C > T) in *SON*, which altered the alanine in position 557 to valine (A557V). SON is a ubiquitously expressed protein, which has a length of 2426 amino acids and is localized in nuclear speckles. The structural features of SON consist of a G-patch domain with RNA-binding function, a double- stranded RNA binding motif (DRBM), a forkhead N-terminal region, an arginine/serine-rich region (RS region) and long repeats of amino acids [85] (**Fig. 21 B**). SON acts as a DNA/RNA-binding protein and mRNA splicing cofactor by enabling the efficient splicing of transcripts with weak splice sites, through ensuring intron removal from the transcripts. The spliced transcripts are essential for cell cycle regulation, DNA repair, apoptosis and epigenetic modifications. Thus, SON is fundamental for cellular function, cell proliferation as well as genomic integrity [85]. Additionally,

SON is relevant for maintaining correct nuclear organization of pre-mRNA processing factors in nuclear speckles and assures their function; SON defects thus disturb cell cycle progression because of disassembly and mislocalization of pre-mRNA processing factors [86]. Not surprisingly, SON alterations have been linked to cancer, such as ductal adenocarcinomas, in which its expression was higher in cancer cells compared to normal duct cells; in this model, knockdown of SON resulted in G2/M arrest and apoptosis progression [87]. Further, alternatively spliced short isoforms of SON were upregulated in acute myeloid leukemia and overexpression of a short isoform was defined as a marker indicating aberrant transcription initiation in leukemia [88]. Therefore, we speculate that the mutation of SON leading to the dysregulation of its many targets caused the very aggressive cancer in our patient.

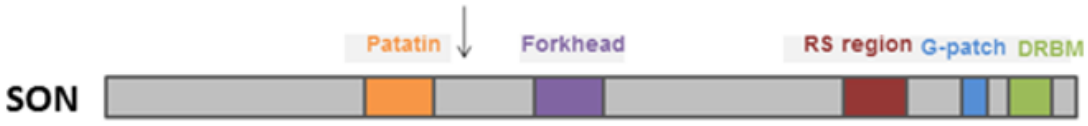

Fig. 21: SON gene structure. Protein domain organization of SON. Black vertical arrows indicate the position of the presented SNV.

In more specific consideration of other potential gene mutations, including those associated with cafe-au-lait spots (NF1, NF2, GNAS1, TSC1 and TSC2, BACH1(FANCJ/BRIP1), FANCA), those associated with hereditary medulloblastoma (APC, BRCA2, CREBBP, EP300, POLE, PTCH1, SMO, TP53), constitutional mismatch repair deficiency syndrome genes (CMMRD) and the SUFU gene, which predisposes to medulloblastoma, we could not identify any SNVs.

These data suggest once more that the mutation in SON likely represents the reason for the uncommon combination of skin alteration and the aggressive brain tumor. However, our whole-exome-based approach cannot exclude, that there are additional mechanisms including epigenetic changes or alterations in non-coding genes, which contribute to the phenotype.

5 Literature

1. Chiu, C., et al., *Mutated SON putatively causes a cancer syndrome comprising high-risk medulloblastoma combined with cafe-au-lait spots.* Fam Cancer, 2019. **18**(3): p. 353-358.
2. Gatta, G., et al., *Childhood cancer survival in Europe 1999-2007: results of EUROCARE-5--a population-based study.* Lancet Oncol, 2014. **15**(1): p. 35-47.
3. Worst, B.C., et al., *Next-generation personalised medicine for high-risk paediatric cancer patients - The INFORM pilot study.* Eur J Cancer, 2016. **65**: p. 91-101.
4. Grobner, S.N., et al., *The landscape of genomic alterations across childhood cancers.* Nature, 2018. **555**(7696): p. 321-327.
5. Dzierzak, E. and A. Bigas, *Blood Development: Hematopoietic Stem Cell Dependence and Independence.* Cell Stem Cell, 2018. **22**(5): p. 639-651.
6. Bhojwani, D., J.J. Yang, and C.H. Pui, *Biology of childhood acute lymphoblastic leukemia.* Pediatr Clin North Am, 2015. **62**(1): p. 47-60.
7. Niemeyer, C. and A. Eggert, *Pädiatrische Hämatologie und Onkologie*. Vol. 2. 2017: Springer-Verlag.
8. Pui, C.H., et al., *Childhood Acute Lymphoblastic Leukemia: Progress Through Collaboration.* J Clin Oncol, 2015. **33**(27): p. 2938-48.
9. Eckert, C., et al., *Use of allogeneic hematopoietic stem-cell transplantation based on minimal residual disease response improves outcomes for children with relapsed acute lymphoblastic leukemia in the intermediate-risk group.* J Clin Oncol, 2013. **31**(21): p. 2736-42.
10. Tallen, G., et al., *Long-term outcome in children with relapsed acute lymphoblastic leukemia after time-point and site-of-relapse stratification and intensified short-course multidrug chemotherapy: results of trial ALL-REZ BFM 90.* J Clin Oncol, 2010. **28**(14): p. 2339-47.
11. Acosta-Maldonado, B.L., et al., *Relapsed ACUTE Leukemia after Hematopoietic STEM CELL Transplantation.* Blood, 2015. **126**(23): p. 5545-54.
12. Sramkova, L., et al., *Detectable minimal residual disease before allogeneic hematopoietic stem cell transplantation predicts extremely poor prognosis in children with acute lymphoblastic leukemia.* Pediatr Blood Cancer, 2007. **48**(1): p. 93-100.
13. Schlegel, P., et al., *Pediatric posttransplant relapsed/refractory B-precursor acute lymphoblastic leukemia shows durable remission by therapy with the T-cell engaging bispecific antibody blinatumomab.* Haematologica, 2014. **99**(7): p. 1212-9.
14. Maude, S.L., et al., *Chimeric antigen receptor T cells for sustained remissions in leukemia.* N Engl J Med, 2014. **371**(16): p. 1507-17.

15. Kato, M., et al., *Second allogeneic hematopoietic SCT for relapsed ALL in children.* Bone Marrow Transplant, 2012. **47**(10): p. 1307-11.

16. Jones, S., et al., *Personalized genomic analyses for cancer mutation discovery and interpretation.* Sci Transl Med, 2015. **7**(283): p. 283ra53.

17. Greaves, M. and C.C. Maley, *Clonal evolution in cancer.* Nature, 2012. **481**(7381): p. 306-13.

18. Torry, D.S. and G.M. Cooper, *Proto-oncogenes in development and cancer.* Am J Reprod Immunol, 1991. **25**(3): p. 129-32.

19. Greenman, C., et al., *Patterns of somatic mutation in human cancer genomes.* Nature, 2007. **446**(7132): p. 153-8.

20. Louis, D.N., et al., *The 2016 World Health Organization Classification of Tumors of the Central Nervous System: a summary.* Acta Neuropathol, 2016. **131**(6): p. 803-20.

21. Roberts, R.O., et al., *Medulloblastoma: a population-based study of 532 cases.* J Neuropathol Exp Neurol, 1991. **50**(2): p. 134-44.

22. Koeller, K.K. and E.J. Rushing, *From the archives of the AFIP: medulloblastoma: a comprehensive review with radiologic-pathologic correlation.* Radiographics, 2003. **23**(6): p. 1613-37.

23. von Bueren, A.O., et al., *Treatment of Children and Adolescents With Metastatic Medulloblastoma and Prognostic Relevance of Clinical and Biologic Parameters.* J Clin Oncol, 2016. **34**(34): p. 4151-4160.

24. Kargl, S., M. Meissl, and W. Pumberger, *Early postnatal diagnosis of Costello syndrome.* Klin Padiatr, 2015. **227**(1): p. 45-7.

25. Wimmer, K. and J. Etzler, *Constitutional mismatch repair-deficiency syndrome: have we so far seen only the tip of an iceberg?* Hum Genet, 2008. **124**(2): p. 105-22.

26. Rosenbaum, T. and K. Wimmer, *Neurofibromatosis type 1 (NF1) and associated tumors.* Klin Padiatr, 2014. **226**(6-7): p. 309-15.

27. Monroe, C.L., S. Dahiya, and D.H. Gutmann, *Dissecting Clinical Heterogeneity in Neurofibromatosis Type 1.* Annu Rev Pathol, 2017. **12**: p. 53-74.

28. Ferner, R.E. and D.H. Gutmann, *Neurofibromatosis type 1 (NF1): diagnosis and management.* Handb Clin Neurol, 2013. **115**: p. 939-55.

29. Evans, D.G., et al., *Malignant peripheral nerve sheath tumours in neurofibromatosis 1.* J Med Genet, 2002. **39**(5): p. 311-4.

30. Orlova, K.A. and P.B. Crino, *The tuberous sclerosis complex.* Ann N Y Acad Sci, 2010. **1184**: p. 87-105.

31. Crino, P.B., K.L. Nathanson, and E.P. Henske, *The tuberous sclerosis complex.* N Engl J Med, 2006. **355**(13): p. 1345-56.

32. Ripperger, T., et al., *Childhood cancer predisposition syndromes-A concise review and recommendations by the Cancer Predisposition*

Working Group of the Society for Pediatric Oncology and Hematology. Am J Med Genet A, 2017. **173**(4): p. 1017-1037.

33. Yang, Y., et al., *Clinical whole-exome sequencing for the diagnosis of mendelian disorders.* N Engl J Med, 2013. **369**(16): p. 1502-11.
34. Hoell, J.I., et al., *Constitutional mismatch repair-deficiency and whole-exome sequencing as the means of the rapid detection of the causative MSH6 defect.* Klin Padiatr, 2014. **226**(6-7): p. 357-61.
35. Hoell, J.I., et al., *Pediatric ALL relapses after allo-SCT show high individuality, clonal dynamics, selective pressure, and druggable targets.* Blood Adv, 2019. **3**(20): p. 3143-3156.
36. Li, H. and R. Durbin, *Fast and accurate long-read alignment with Burrows-Wheeler transform.* Bioinformatics, 2010. **26**(5): p. 589-595.
37. Li, H., et al., *The Sequence Alignment/Map format and SAMtools.* Bioinformatics, 2009. **25**(16): p. 2078-9.
38. Duraku, L.S., et al., *Re-innervation patterns by peptidergic Substance-P, non-peptidergic P2X3, and myelinated NF-200 nerve fibers in epidermis and dermis of rats with neuropathic pain.* Exp Neurol, 2013. **241**: p. 13-24.
39. Gomes, B., et al., *Variations in the quality and costs of end-of-life care, preferences and palliative outcomes for cancer patients by place of death: the QUALYCARE study.* BMC Cancer, 2010. **10**: p. 400.
40. DePristo, M.A., et al., *A framework for variation discovery and genotyping using next-generation DNA sequencing data.* Nat Genet, 2011. **43**(5): p. 491-8.
41. *Broad Institute*. 2021 30.05.2021; Available from: https://www.broadinstitute.org/.
42. McLaren, W., et al., *Deriving the consequences of genomic variants with the Ensembl API and SNP Effect Predictor.* Bioinformatics, 2010. **26**(16): p. 2069-70.
43. Adzhubei, I.A., et al., *A method and server for predicting damaging missense mutations.* Nat Methods, 2010. **7**(4): p. 248-9.
44. Kumar, P., S. Henikoff, and P.C. Ng, *Predicting the effects of coding non-synonymous variants on protein function using the SIFT algorithm.* Nat Protoc, 2009. **4**(7): p. 1073-81.
45. Cibulskis, K., et al., *Sensitive detection of somatic point mutations in impure and heterogeneous cancer samples.* Nat Biotechnol, 2013. **31**(3): p. 213-9.
46. Koboldt, D.C., et al., *VarScan 2: somatic mutation and copy number alteration discovery in cancer by exome sequencing.* Genome Res, 2012. **22**(3): p. 568-76.
47. *HUGO Gene Nomenclature Committee*. 2021; Available from: https://www.genenames.org/.

48. Warmuth, M., et al., *Ba/F3 cells and their use in kinase drug discovery.* Curr Opin Oncol, 2007. **19**(1): p. 55-60.

49. Mercimek-Mahmutoglu, S., et al., *Thirteen new patients with guanidinoacetate methyltransferase deficiency and functional characterization of nineteen novel missense variants in the GAMT gene.* Hum Mutat, 2014. **35**(4): p. 462-9.

50. Kinzel, D., et al., *Pitchfork regulates primary cilia disassembly and left-right asymmetry.* Dev Cell, 2010. **19**(1): p. 66-77.

51. McIntyre, J.C., C.L. Williams, and J.R. Martens, *Smelling the roses and seeing the light: gene therapy for ciliopathies.* Trends Biotechnol, 2013. **31**(6): p. 355-63.

52. Conduit, S.E., et al., *A compartmentalized phosphoinositide signaling axis at cilia is regulated by INPP5E to maintain cilia and promote Sonic Hedgehog medulloblastoma.* Oncogene, 2017. **36**(43): p. 5969-5984.

53. *Annual report German childhood cancer registry*. 2015 17.07.2020]; Available from: http://www.kinderkrebsregister.de/typo3temp/secure_downloads/29942/0/f474d594c6b5a8805c4e629db249872e05d69ddb/jb2015_s.pdf.

54. Fischer, U., et al., *Genomics and drug profiling of fatal TCF3-HLF-positive acute lymphoblastic leukemia identifies recurrent mutation patterns and therapeutic options.* Nat Genet, 2015. **47**(9): p. 1020-9.

55. Mullighan, C.G., et al., *Genome-wide analysis of genetic alterations in acute lymphoblastic leukaemia.* Nature, 2007. **446**(7137): p. 758-64.

56. *Cosmic Database*. 2021 18.06.2021; Available from: https://cancer.sanger.ac.uk/cosmic/gene/analysis?ln=NRAS.

57. Dogan, S., et al., *Molecular epidemiology of EGFR and KRAS mutations in 3,026 lung adenocarcinomas: higher susceptibility of women to smoking-related KRAS-mutant cancers.* Clin Cancer Res, 2012. **18**(22): p. 6169-77.

58. Kanda, M., et al., *Presence of somatic mutations in most early-stage pancreatic intraepithelial neoplasia.* Gastroenterology, 2012. **142**(4): p. 730-733 e9.

59. Hingorani, S.R., et al., *Preinvasive and invasive ductal pancreatic cancer and its early detection in the mouse.* Cancer Cell, 2003. **4**(6): p. 437-50.

60. Smagulova, K.K., D.R. Kaydarova, and T.S. Nasrytdinov, *[The study of rate and spectrum of frequency of mutations of gene KRAS in patients with colorectal cancer in the Republic of Kazakhstan].* Probl Sotsialnoi Gig Zdravookhranenniiai Istor Med, 2020. **28**(1): p. 134-138.

61. Hu, Y., et al., *Prognostic Value of NRAS Gene for Survival of Colorectal Cancer Patients: A Systematic Review and Meta-Analysis.* Asian Pac J Cancer Prev, 2018. **19**(11): p. 3001-3008.

62. Demin, D.E., et al., *Constitutive Expression of NRAS with Q61R Driver Mutation Activates Processes of Epithelial-Mesenchymal Transition and Leads to Substantial Transcriptome Change of Nthy-ori 3-1 Thyroid Epithelial Cells.* Biochemistry (Mosc), 2019. **84**(4): p. 416-425.

63. Liang, D.C., et al., *K-Ras mutations and N-Ras mutations in childhood acute leukemias with or without mixed-lineage leukemia gene rearrangements.* Cancer, 2006. **106**(4): p. 950-6.

64. Prieto, C., et al., *Activated KRAS Cooperates with MLL-AF4 to Promote Extramedullary Engraftment and Migration of Cord Blood CD34+ HSPC But Is Insufficient to Initiate Leukemia.* Cancer Res, 2016. **76**(8): p. 2478-89.

65. Li, T.T., et al., *[NRAS Gene Expression and Its Clinical Significance in Patients with Acute Myeloid Leukemia].* Zhongguo Shi Yan Xue Ye Xue Za Zhi, 2020. **28**(1): p. 76-81.

66. Matsuda, K., et al., *Spontaneous improvement of hematologic abnormalities in patients having juvenile myelomonocytic leukemia with specific RAS mutations.* Blood, 2007. **109**(12): p. 5477-80.

67. Bello, M., J. Correa-Basurto, and M.A. Vargas-Mejia, *Molecular mechanism of the association and dissociation of Deltarasin from the heterodimeric KRas4B-PDEdelta complex.* Biopolymers, 2019. **110**(11): p. e23333-47.

68. Infante, J.R., et al., *Safety, pharmacokinetic, pharmacodynamic, and efficacy data for the oral MEK inhibitor trametinib: a phase 1 dose-escalation trial.* Lancet Oncol, 2012. **13**(8): p. 773-81.

69. Irving, J., et al., *Ras pathway mutations are prevalent in relapsed childhood acute lymphoblastic leukemia and confer sensitivity to MEK inhibition.* Blood, 2014. **124**(23): p. 3420-3430.

70. Scagliotti, G.V., S. Novello, and J. von Pawel, *The emerging role of MET/HGF inhibitors in oncology.* Cancer Treat Rev, 2013. **39**(7): p. 793-801.

71. Birchmeier, C., et al., *Met, metastasis, motility and more.* Nat Rev Mol Cell Biol, 2003. **4**(12): p. 915-25.

72. Harshman, L.C. and T.K. Choueiri, *Targeting the hepatocyte growth factor/c-Met signaling pathway in renal cell carcinoma.* Cancer J, 2013. **19**(4): p. 316-23.

73. Okuma, H.S. and S. Kondo, *Trends in the development of MET inhibitors for hepatocellular carcinoma.* Future Oncol, 2016. **12**(10): p. 1275-86.

74. Paik, P.K., et al., *Response to MET inhibitors in patients with stage IV lung adenocarcinomas harboring MET mutations causing exon 14 skipping.* Cancer Discov, 2015. **5**(8): p. 842-9.

75. Sadiq, A.A. and R. Salgia, *MET as a possible target for non-small-cell lung cancer.* J Clin Oncol, 2013. **31**(8): p. 1089-96.

76. Feng, Y. and P.C. Ma, *MET targeted therapy for lung cancer: clinical development and future directions.* Lung Cancer (Auckl), 2012. **3**: p. 53-67.

77. Janic, D., et al., *Application of targeted next generation sequencing for the mutational profiling of patients with acute lymphoblastic leukemia.* J Med Biochem, 2020. **39**(1): p. 72-82.

78. Cante-Barrett, K., et al., *MEK and PI3K-AKT inhibitors synergistically block activated IL7 receptor signaling in T-cell acute lymphoblastic leukemia.* Leukemia, 2016. **30**(9): p. 1832-43.

79. White, Y., et al., *KRAS insertion mutations are oncogenic and exhibit distinct functional properties.* Nat Commun, 2016. **7**: p. 10647-55.

80. Kuribara, R., et al., *Two distinct interleukin-3-mediated signal pathways, Ras-NFIL3 (E4BP4) and Bcl-xL, regulate the survival of murine pro-B lymphocytes.* Mol Cell Biol, 1999. **19**(4): p. 2754-62.

81. Schmidt, L., et al., *Novel mutations of the MET proto-oncogene in papillary renal carcinomas.* Oncogene, 1999. **18**(14): p. 2343-50.

82. de Aguirre, I., et al., *c-Met Mutational Analysis in the Sema and Juxtamembrane Domains in Small-Cell-Lung-Cancer.* Transl Oncogenomics, 2006. **1**: p. 11-8.

83. Ma, P.C., et al., *c-MET mutational analysis in small cell lung cancer: novel juxtamembrane domain mutations regulating cytoskeletal functions.* Cancer Res, 2003. **63**(19): p. 6272-81.

84. *INFORM Registry*. 21.06.2021; Available from: https://www.dkfz.de/en/inform/.

85. Hickey, C.J., J.H. Kim, and E.Y. Ahn, *New discoveries of old SON: a link between RNA splicing and cancer.* J Cell Biochem, 2014. **115**(2): p. 224-31.

86. Sharma, A., et al., *Son is essential for nuclear speckle organization and cell cycle progression.* Mol Biol Cell, 2010. **21**(4): p. 650-63.

87. Furukawa, T., et al., *Targeting of MAPK-associated molecules identifies SON as a prime target to attenuate the proliferation and tumorigenicity of pancreatic cancer cells.* Mol Cancer, 2012. **11**: p. 88.

88. Kim, J.H., et al., *SON and Its Alternatively Spliced Isoforms Control MLL Complex-Mediated H3K4me3 and Transcription of Leukemia-Associated Genes.* Mol Cell, 2016. **61**(6): p. 859-73.

Acknowledgements

Special thanks are given to Prof. Dr. A. Borkhardt and PD Dr. J. Höll for their advice on the content and form of this thesis.

This work was funded by Düsseldorf School of Oncology (DSO) of Heinrich Heine University Düsseldorf.